iScience

CellPress
OPEN ACCESS

Article

Riboproteome remodeling during quiescence exit in *Saccharomyces cerevisiae*

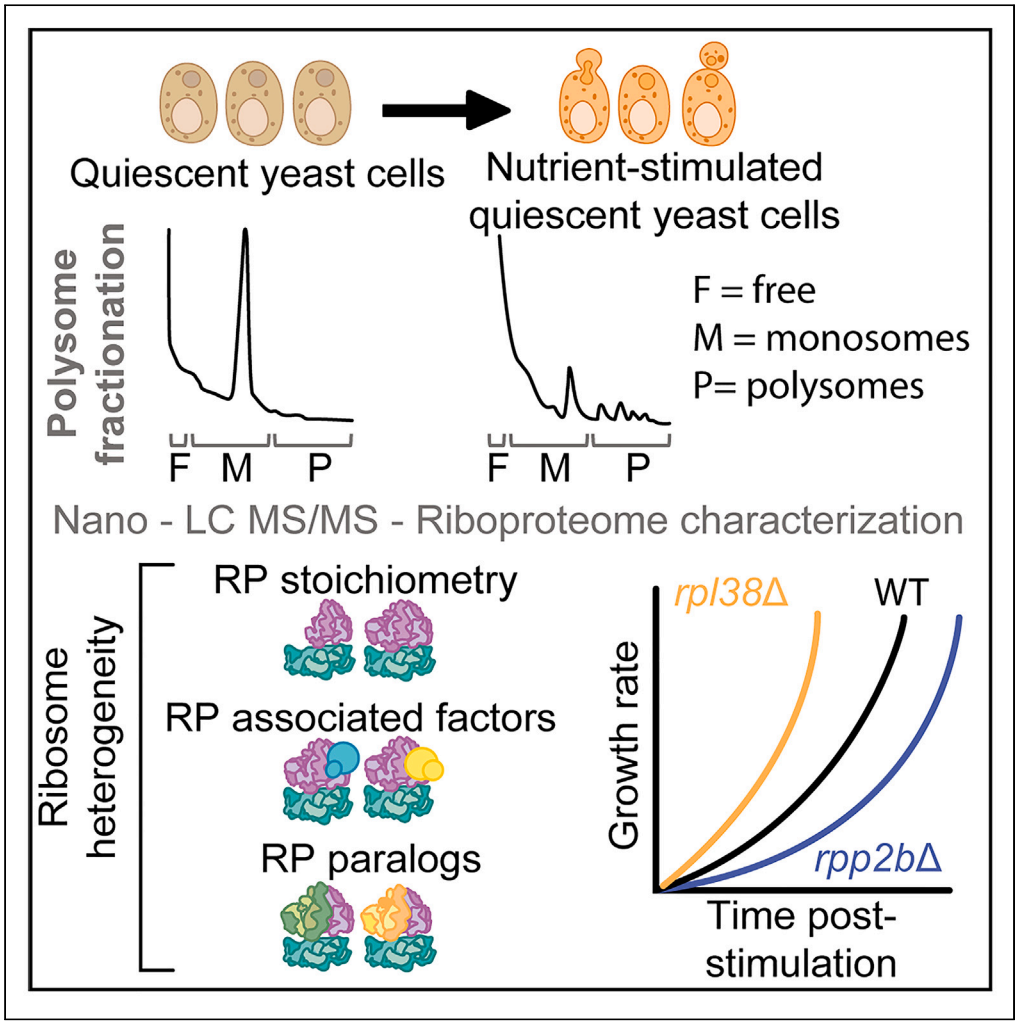

Clara A. Solari, María Clara Ortolá Martínez, Juan M. Fernandez, ..., Silvia Rossi, Mark P. Ashe, Paula Portela

pportela@qb.fcen.uba.ar

Highlights

Quiescent yeast cells contain ribosomes with different compositions

The ribosome composition varies between monosomes and polysomes during quiescence exit

Ribosome composition can result in changes in translational activity

Solari et al., iScience 27, 108727
January 19, 2024 © 2023
https://doi.org/10.1016/j.isci.2023.108727

iScience

CellPress
OPEN ACCESS

Article

Riboproteome remodeling during quiescence exit in *Saccharomyces cerevisiae*

Clara A. Solari,[1] María Clara Ortolá Martínez,[1] Juan M. Fernandez,[1] Christian Bates,[4] Gerardo Cueto,[2] María Pía Valacco,[3] Fabián Morales-Polanco,[4,5] Silvia Moreno,[3] Silvia Rossi,[1] Mark P. Ashe,[4] and Paula Portela[1,6,*]

SUMMARY

The quiescent state is the prevalent mode of cellular life in most cells. *Saccharomyces cerevisiae* is a useful model for studying the molecular basis of the cell cycle, quiescence, and aging. Previous studies indicate that heterogeneous ribosomes show a specialized translation function to adjust the cellular proteome upon a specific stimulus. Using nano LC-MS/MS, we identified 69 of the 79 ribosomal proteins (RPs) that constitute the eukaryotic 80S ribosome during quiescence. Our study shows that the riboproteome is composed of 444 accessory proteins comprising cellular functions such as translation, protein folding, amino acid and glucose metabolism, cellular responses to oxidative stress, and protein degradation. Furthermore, the stoichiometry of both RPs and accessory proteins on ribosome particles is different depending on growth conditions and among monosome and polysome fractions. Deficiency of different RPs resulted in defects of translational capacity, suggesting that ribosome composition can result in changes in translational activity during quiescence.

INTRODUCTION

The regulation of protein translation is essential for proteome adaptation to nutrient availability, cell differentiation, growth, and organismal development.[1] Heterogeneity in ribosomal composition can lead to ribosome specialization contributing to translational regulation by modifications to either the ribosomal core particle or ribosome-associated proteins.[2] Overall, the eukaryotic ribosome is composed of a large 60S subunit, consisting of three rRNAs (25S, 5.8S, 5S) and 46 different ribosomal proteins (RPs), and a small 40S subunit, consisting of 18S rRNA and 33 RPs.[3] Ribosomes may vary in composition at the level of core RPs and/or accessory proteins, leading to the formation of ribosomal populations with different functions and capacities that ultimately modulate translation. Such ribosomal heterogeneity can be brought about by changes in RP stoichiometry,[4] differences between RP paralogs,[5–7] presence/absence of RPs,[8] presence/absence of ribosome associated-factors,[9] and post-translational modifications of RPs or auxiliary factors.[10,11] The rRNA also provides ribosome variability, as there is substantial diversity in the rRNA sequence and its post-transcriptional modification.[12–14]

Ribosome heterogeneity, caused by the incorporation of different RP paralogs, has been observed in diverse organisms.[15–18] In *Saccharomyces cerevisiae*, 37 of the 59 duplicated RP genes have one or more amino acid differences.[19] Studies of ribosome heterogeneity in yeast also demonstrate the presence of populations of ribosomes differentially assembled with non-identical ribosomal protein paralogs in response to stress.[7]

In addition to modifications of the ribosome core protein composition, the ribosome has ribosome-associated proteins that also confer specialized functions. These associated proteins interact with ribosomes through the ribosome surface and have various functions on post and co-translational proteostasis.[20,21] One of these interactions is mediated by rRNA expansion segments which differ markedly between species.[22] In the eukaryotic ribosome the scaffold expansion segment ES27L (largest ESs of the 25S rRNA) recruits the N-terminal segment of a methionine aminopeptidase enzyme which regulates translation fidelity.[23] In *S. cerevisiae*, Asc1 (RACK1 in humans), Rps2, Rps3, and Rps20 form an exposed point of contact in the head region of the ribosomal 40S subunit. This area interacts with protein factors involved in several processes including the ubiquitination-deubiquitination of ribosomal proteins, clamping of inactive ribosomal subunits, mRNA surveillance and vesicular transport, mRNA degradation, autophagy, and kinase signaling.[24] The importance of tissue-specific ribosome

[1]Universidad de Buenos Aires, Facultad de Ciencias Exactas y Naturales, Departamento de Química Biológica, Instituto de Química Biológica de la Facultad de Ciencias Exactas y Naturales-Consejo Nacional de Investigaciones Científicas y Técnicas (IQUIBICEN-CONICET), Buenos Aires, Argentina
[2]Universidad de Buenos Aires, Facultad de Ciencias Exactas y Naturales, Departamento de Ecología, Genética y Evolución, Instituto IEGEBA (CONICET-UBA), Buenos Aires, Argentina
[3]CEQUIBIEM- Universidad de Buenos Aires, Facultad de Ciencias Exactas y Naturales, Departamento de Química Biológica, Instituto de Química Biológica de la Facultad de Ciencias Exactas y Naturales-Consejo Nacional de Investigaciones Científicas y Técnicas (IQUIBICEN-CONICET), Buenos Aires, Argentina
[4]The Michael Smith Building, Faculty of Life Sciences, University of Manchester, Manchester, UK
[5]Present address: Department of Biological Sciences, Stanford University, 318 Campus Drive, Stanford CA 94305, USA
[6]Lead contact
*Correspondence: pportela@qb.fcen.uba.ar
https://doi.org/10.1016/j.isci.2023.108727

specialization is evident in the ribosomopathies which result from mutations in RP genes. These mutations affect ribosome abundance and/or function producing phenotypic effects in specific tissues, such as bone marrow-derived lineages[25,26] and skeletal tissues.[27]

In *S. cerevisiae*, the population of ribosomes changes according to growth conditions and metabolic state. For instance, the switch from glucose to glycerol growth promotes an increase in 80S ribosomes lacking Rpl10, Rps1, Rps14 A/B, and Rps26 A/B.[28] Moreover, the paralog Rpl1B from the Rpl1A/B pair improves the translational efficiency of mitochondrial proteins under respiratory metabolism.[6] In addition, the RP stoichiometry is dependent on the quantity of ribosomes per mRNA in response to ethanol or a low glucose content.[29]

The ratios between the polysomal and monosomal levels of RPs paralogs are conserved between yeast and mouse orthologs.[29] During osmotic stress, duplicated ribosomal protein genes are differentially expressed modifying the proportion of ribosomes carrying a specific paralog.[7] Rps26 depleted ribosomes are produced under alkaline pH or high salt concentrations, and these ribosomes show a preference for mRNAs with deviations at the Kozak sequence leading to changes in the proteome.[30]

In addition, the ribosome-associated proteins also contribute to ribosome heterogeneity and specialization. For instance, the late-annotated small open reading frame (Lso2) interacts with the ribosome close to the GTPase activation core, and is required for translation activation during recovery from the stationary phase.[31]

Quiescence is a reversible cellular transitory growth pause in which cells can resume cell growth and division in response to stimulation. In yeast and mammalian cells, the quiescent state shares key characteristics including an arrest of the cell cycle, condensation of chromosomes, reduction in the synthesis of ribosomal RNA, protein translation arrest, decrease in cell size, activation of autophagy, and an increase in resistance to various stresses.[32]

Pioneering studies in *S. cerevisiae* determined that quiescent yeast cells show decreased global protein translation[33] but survival in this state requires the upregulation of proteins that function as stress protectants, such as chaperones and heat shock proteins.[34,35] This reduction in protein translation that occurs during quiescence could be a consequence of the decrease in the transcription of RP genes,[36] and also a reduction in the translation of specific translation initiation factors such as eIF4E, eIF4G, and Rpg1,[37,38] although it is also possible that signaling pathways act to dampen protein synthesis.[39] Quiescent yeast cells also remodel and reorganize macromolecular structures and organelles.[40] mRNA-processing enzymes relocalize to SGs and PBs and there is evidence that these foci are important for long-term survival in the stationary phase.[41,42] Stationary phase mRNPs appear distinct from the PBs and SGs evoked by heat stress or glucose starvation.[42–44] Closer inspection of the protein composition of mRNP foci from the stationary phase, shows the presence of some typical PB and SG protein components, as well as both small and large ribosomal subunit components e.g., the Rps3 and Rpl35A ribosomal proteins.[38] When nutrients become available, the mRNP foci observed in quiescent cells are quickly disassembled,[40] transcription is reactivated,[45,46] protein translation gradually resumes[31,38] and cells re-enter a proliferative phase.[40]

It is still unclear how the regulation of protein translation controls the proteome homeostasis during the transition from quiescence to growth. Here, we analyze the composition of the riboproteome during the initial events surrounding exit from quiescence using a mass spectrometry-based proteomics approach in yeast cells. We show that RP stoichiometry in both monosomal and polysomal fractions changes depending on growth conditions. We also identify a specific repertoire of previously reported ribosome-associated proteins including proteasome proteins, co-translational acting chaperones, proteins for ribosome subunit stabilization, translation factors, and mRNA-binding proteins. We further characterize how the lack of certain RP proteins affect the translational activity, suggesting that differences in ribosome protein composition regulates the translational activity during the exit from the quiescent state in yeast.

RESULTS

Characterization of translation features in nutrient-stimulated quiescent cells

We characterized the translational state during a time course of nutrient stimulation of quiescent cells. To this end, we measured the global translational state of the cells, the mRNA and protein levels of quiescence exit markers. The global protein translation status was measured using polysomal profile analysis on extracts prepared from stationary phase cells (OD_{600} = 8; t = 72 h), after the addition of a nutrient stimulus during 30-, 60-, and 150 min and also from cells in exponential phase (OD_{600} = 0.6; t = 6 h) (Figures 1A and S1A). This analysis shows that most of the ribosomes from quiescent cells fractionated as 80S monosomes (ratio monosome/polysome = 17 $\pm$ 1.3), consistent with the described global reduction of translation initiation, in chronologically aged yeast cells.[47,48] Addition of nutrient rich media promoted a gradual increase in global protein translation as shown by the shift of ribosomes from the monosomal to the polysomal fractions. At 30 min after the addition of fresh media there was a slight translational reactivation (ratio monosome/polysome = 3.1 $\pm$ 0.1), but in the following 60 or 150 min the gradient profiles resemble those from exponential cells (ratio monosome/polysome = 0.74 $\pm$ 0.01; 0.57 $\pm$ 0.08; 0.16 $\pm$ 0.02 respectively) (Figure 1A).

To analyze whether the global protein translation reactivation upon exit from quiescence correlates with an increase in the overall ribosome content, the abundances of 25S and 18S rRNAs, and Rps3 (small 40S subunit RP) and Rpl35 A/B (large 60S subunit RP) ribosomal proteins were measured from stationary phase cells before and after the stimulation with fresh medium. The levels of the rRNAs and the RPs analyzed show no change following stimulation for 30 or 60 min (Figures S1B and S1C). We extended the analysis to several others RPs, and most show no change in their level comparing pre and post stimulated quiescent cells (Figure S5). However, an increase in the levels of these proteins was detected after 2.5 h post-stimulation (data not shown). All of the RPs expressed in quiescent and stimulated cells are probably assembled into ribosomal particles, since no protein was detected in the non-ribosomal fractions from sucrose sedimentation gradients. (Figure S4B; Table S1). These results suggest that the translation resumption occurring upon exit from quiescence relies upon a preserved pool of ribosomes.

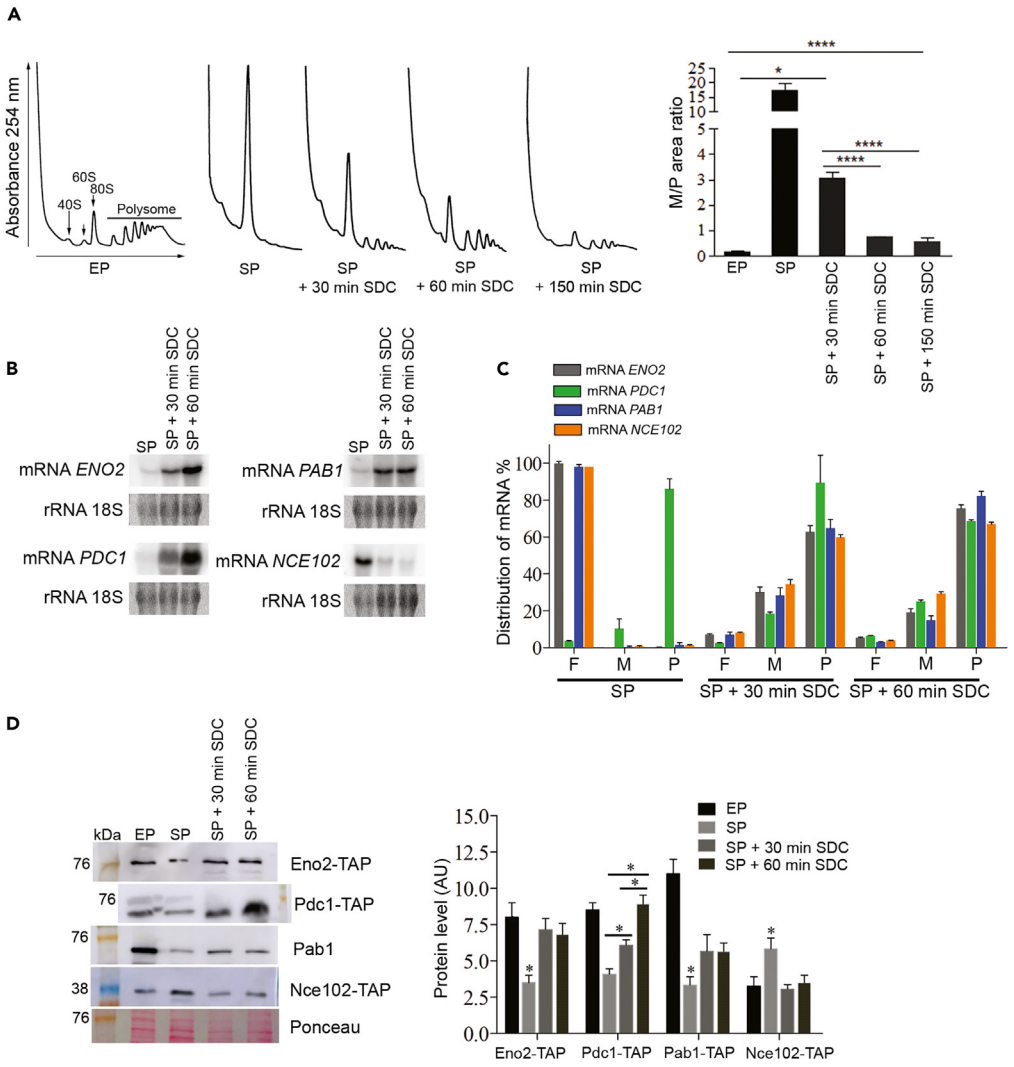

Figure 1. Global translational state of quiescent cells before and after stimulation with nutrients

(A) $A_{254\ nm}$ traces show the polysome profiles of cells in exponential phase (EP), in stationary phase (SP) or after stimulation with fresh medium for 30 min (SP + 30 min SDC), 60 min (SP + 60 min SDC) and 150 min (SP + 150 min SDC). The 40S, 60S, 80S particles, and polysomes are indicated. Equal amounts of total RNA were used in each gradient. The graph shows the 80S (M)/polysome (P) area, mean ± SE n = 3 biological replicates. Statistical significance was determined with a one-way ANOVA test and Tukey contrasts test (*p < 0.001; ****p < 0.0001). n = 3 biological replicates.

(B) mRNA levels and (C) distribution in polysomal profiles during quiescence and after fresh medium stimulation. Total mRNAs were measured by Northern blot from cells in the stationary phase (SP) and after 30 min (SP + 30 min SDC) or 60 min (SP + 60 min SDC) of stimulation with fresh medium. 18S rRNA was used as a loading control. mRNA distribution in polysome profile was performed in 15–50% sucrose gradient fractions in SP, SP + 30 min SDC, or SP + 60 min SDC. Samples were pooled depending on the ribosomal content: free are fractions with densities less than 40S (F); monosomal are fractions between 40S and 80S (M), polysomal are fractions over 80S (P); as indicated in the example polysomal profile on the left. The percentage distribution of *ENO2*, *PDC1*, *PAB1* and *NCE102* mRNAs in each fraction measured by RT-qPCR was plotted. Luciferase mRNA was used as a control. The values represent the mean ± SE, n = 2 biological replicates.

(D) Protein levels of ENO2-TAP, PDC1-TAP, Pab1, and NCE102-TAP during exponential growth (EP), stationary phase (SP), and after 30 min or 60 min of stimulation with fresh medium (SP + 30 min SDC or SP + 60 min SDC) were determined by Western blot using anti-TAP or anti-Pab1p antibodies. Ponceau red was used as a loading control. Quantification of Western blot was performed by densitometry (mean ± SE, n = 3 biological replicates). Statistical significance for each protein was determined with a one-way ANOVA and the Tukey contrast test ****p < 0.0001.

In order to further analyze the translational reactivation in nutrient-stimulated quiescent cells, we assessed the mRNA polysome association and protein levels of selected proteins from pre- and post-stimulated quiescent cells. *NCE102*, *ENO2*, *PDC1* and *PAB1* mRNAs were chosen and considered as "mRNA markers" as they encode proteins that play important roles in preserving quiescence or cell proliferation once nutrients are available.[49–54] As previously described,[38,55] *ENO2*, *PDC1*, and *PAB1* mRNA levels are low in the stationary phase and increase after nutrient stimulation, while *NCE102* mRNA shows the opposite behavior (Figure 1B). In addition, during quiescence, when global

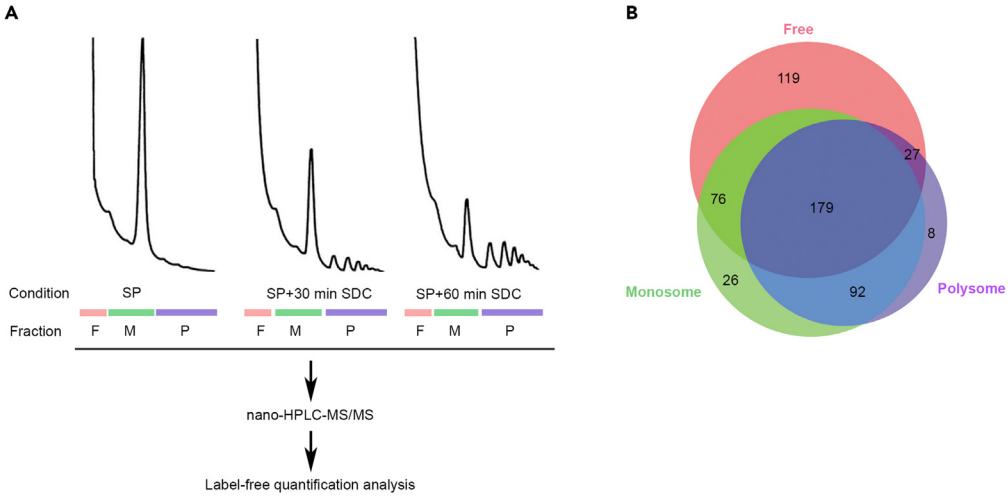

Figure 2. Riboproteome characterization during quiescence and translational recovery

(A) Experimental design of the proteomic screen. Stationary phase (SP) cells were harvested by centrifugation and resuspended in the same volume of fresh medium for 30 min (SP + 30 min SDC), or 60 min (SP + 60 min SDC). Free (F), monosomal (M, 40S + 60S + 80S), and polysomal (P) fractions were obtained by ultracentrifugation through sucrose gradients and analyzed by nanoLC-MS/MS (for details, see STAR Methods).

(B) Distribution of 527 total proteins detected in all 3 growth conditions through mass spectrometry. The number of proteins for each subgroup is indicated. See also Figure S3.

translation is arrested, (Figure 1A), *ENO2, PAB1* and *NCE102* mRNAs are present in the ribosome-free fractions of sucrose gradients (Figure 1C). However, 60%–80% of these mRNAs are present in polysomal fractions after 30 to 60 min of nutritional stimulation, (Figure 1C). On the other hand, the *PDC1* mRNA remains mainly associated with the polysome fractions both in quiescent and stimulated cells (Figure 1C). Given that the 5′ UTR (untranslated region) of *PDC1* mRNA is shorter than the average found in *S. cerevisiae*,[56] it is possible that *PDC1* mRNA translation initiation persists under conditions of global repression, competing more effectively for limiting translation factors.

Finally, the correlation between translation, mRNA levels, and protein levels was assessed. The protein levels were evaluated by Western blot using TAP-tagged strains[57] (Figure 1D). Three protein expression patterns were observed: (i) Pab1 and Eno2 show an increase in protein levels correlating with the increased levels of mRNA, and the association of these mRNAs with polysomes in cells post-stimulus; (ii) both *PDC1* mRNA and protein levels are increased after stimulus, but the percentage of mRNA association with polysomes remained similar to the one observed from stationary phase cells (≈80%) or nutrient stimulus cells, (iii) both *NCE102* mRNA and protein levels decreased after fresh media stimulation. This decrease in protein levels seems to be a consequence of changes in protein synthesis, since the protein turnover rate is similar in quiescent and stimulated cells (t 1/2 > 120 min, Figure S2). This higher level of Nce102 protein under stationary phase conditions, where there is a global inhibition of translational initiation, could be a consequence of post-translational mechanisms, as the protein is specifically sequestered into eisosomes.[58]

Overall, these results indicate that during the first 60 min after the nutrient stimulation of quiescent cells the cellular proteome changes as a consequence of translational activation either at the global or mRNA specific level without changes in total ribosome content. Most recently, the role of specialized ribosomes as a mechanism that controls proteome adaptation following environmental change has gained significant attention.[59–61] However, variations in yeast ribosome composition during the exit from quiescence have not been examined yet.

Characterization of the riboproteome composition in quiescent cells and post-translational reactivation

To characterize ribosome heterogeneity during the exit from quiescence, the protein composition of ribosomal particles from stationary phase and nutrient-stimulated cells was assessed. More specifically, a label-free quantitative mass spectrometry strategy was taken to compare quiescent yeast cells with cells that had been nutrient stimulated for 30 and 60 min. To this end, crude extracts from these cells were subjected to sucrose gradient centrifugation, and three fractions, free (F); monosome (M = 80S + 60S + 40S) and polysome (P), were analyzed by nano-HPLC-MS/MS (Figure 2A).

A total of 527 proteins were identified; 45% of identified proteins had already been detected in previous proteomic assays of total protein extracts from stationary phase yeast cells.[51] Among them, 16% of the 527 proteins were ribosomal proteins, although a number of unique and common proteins were identified in each dataset (Figure 2B). For instance, 26 proteins were detected exclusively in monosome fractions, and 8 proteins were unique to polysome fractions.

Discriminant analysis was employed to assess the riboproteome composition obtained through mass spectrometry. Two discriminant functions, accounting for 33% of the total variance, enabled the differentiation of the riboproteome composition among F, M, and P fractions (Figure S3A). This result shows that in addition to the expected differences between the free fraction and ribosomal fractions, there are also compositional differences between monosome and polysome fractions. When the data from the different growth conditions (stationary

phase, 30 min and 60 min after stimulation, Figure S3B) are considered, samples stimulated for 30 min appear intermediate in terms of variability when compared with the stationary phase and 60 min stimulated samples. These findings imply that the protein composition of each fraction changes in response to the nutrient stimulus. Based on these results, we decided to explore the riboproteome data from quiescent cells and cells after 60 min of stimulation with fresh media.

Protein-protein interaction networks analysis for the proteins identified from the monosomal and polysomal fractions from stationary phase and 60 min stimulated samples shows that ribosomal proteins conform to a cluster that is present in all of the networks (Figure S3C). The proteins nearest to the ribosomal protein cluster are involved in protein level maintenance, such as translation and protein folding. It should be noted that the proteasome category is only found in the monosome fractions. Groups related to other cellular processes such as glycolysis, amino acid biosynthesis, oxidative stress, and mitochondria are also found.

From the mass spectrometric identification of proteins, the proteome from free monosome and polysomes fractions was classified into the following 8 functional groups: 1. ribosomal particle, 2. physically associated with ribosomes (ribosome-associated proteins), 3. ribosomal biogenesis, 4. translation, 5. proteasome, 6. protein folding, 7. carbon metabolism and 8. Miscellaneous (Table S1). Analysis of the peptides from the mass spectrometry profiles indicated no bias in the peptide distribution across the primary sequence for individual proteins (data not shown). This result indicates that the detected proteins are likely fully translated proteins that co-fractionate with ribosomes. Using the MS data, we analyzed how the relative abundance of the identified proteins changed across the free, monosome, and polysome fractions during the exit from quiescence (Table S1).

Characterization of ribosome composition

From our proteome analysis, we identified 69 of the expected 79 ribosomal proteins that constitute the 80S ribosome,[3] in the monosomal and polysomal fractions, but not in the free fraction (Table S1). Note that, in the Western blot experiment (Figure S4B), we found very faint bands corresponding to ribosomal proteins in the free fraction, despite the fact that the free fraction had a significantly larger total protein concentration than the monosome and polysome fractions. This result indicates that the majority of RPs detected in our analysis are presumably found as part of functional and fully assembled ribosomes. We found 18 of the 20 ribosomal proteins encoded by single-copy genes and 51 of the 59 ribosomal proteins encoded by paralogous pairs of genes whose homology varies from 78 to 100%.[19] We found 14 pairs of ribosomal proteins paralogs with 100% identity. From non-identical paralogs, 14 pairs were identified by the presence of unique peptides and 8 were identified by peptides coming from only one of the pair of proteins. It was not possible to distinguish between the other 15 paralogs pairs (Figures S4A and S5A). To analyze how the core ribosome composition changes during the translation activation of quiescent cells, we first determined the protein abundance of each RP identified in our experiment (Figure S5A). We observed that all RPs are equally abundant in both quiescent and fresh media-stimulated cells in agreement with our Western blot experiments (Figures S1C and S6). Inspection of the relative expression of the detectable RP paralogous pairs is shown in Figure S5B (Paralog A/B abundance ratio). The proteins of 5 paralogs pairs, showed similar abundance ratios in the ribosome particle: Rps1A/B; Rps21 A/B; Rpl6A/B; Rpl7A/B and Rpl33 A/B. The other 6 detectable paralogous pairs showed that one of the RP proteins was overrepresented: Rps7A/B; Rps9A/B; Rpl21 A/B; Rpl26 A/B; Rpl16 A/B and the pair Rpp2A/B showed a higher proportion of B than A paralog (B is called "major protein paralog"); whereas, Rpl15 A/B; Rpl17 A/B and Rpl24 A/B showed a higher level of A than B paralog (A is called "major protein paralog"). The hierarchy of RP paralog expression during quiescent exit shown here differs from that described in cells under normal and stress growth conditions.[7]

According to earlier research,[45] stationary phase mRNA relative levels for each of the RP paralogs in a pair, exhibit similar abundances (Figure S5C). Taking into account the results shown in Figure S5A, we can see that not all of the RP paralogous pairs exhibit a correlation between their mRNA and protein levels in the stationary phase. We speculate that a paralog-specific post-transcriptional mechanism in both quiescent and exit cells may be responsible for determining the expression pattern of these paralogs.

Our next aim was to investigate whether there were any obvious changes in ribosome composition. For this we analyzed the relative abundance of each RP in monosome and polysome fractions in quiescent cells relative to cells that had been nutrient stimulated for 60 min (Figure 3). 69 ribosomal proteins were identified across the samples, with 25 RPs showing changes in their distribution across different fractions or growth conditions. The results are summarized in Table 1.

For 6 of the paralogous pairs (Rpl17 A/B; Rpl21 A/B; Rps7A/B; Rpl26 A/B; Rps1A/B; Rpl15 A/B) and Rpp2A/B pair, one of the specific RP paralogs was more associated with the ribosomes from either monosome or polysome fractions (Figure 3). There are several paralogous pairs that, regardless of the nutrient stimulus, showed no changes in polysome or monosome fractions (Rpl24 A/B, Rpl33 A/B, Rpl7A/B, Rpl6A/B, Rps21 A/B, and Rps9A/B) (Table S1). Figures 3 and S5B show that there is no correlation between the relative expression levels of paralogs and their preference for polysome incorporation.

To demonstrate the coexistence of a heterogeneous population of ribosomes conformed by different paralogs, we constructed strains co-expressing endogenously tagged Rps7A-HA and Rps7B-GST (Figure S7A) and Rpl16A-GST and Rpl16B-HA (Figure S8A). Both strains show similar protein levels of both paralogs in quiescent and post stimulus cells (Figures S7A and S8A). To corroborate that the HA- and GST-tagged RPs are incorporated into ribosomes resembling endogenous RPs, sucrose cushion fractions were assessed by Western blot analysis. Both Rps7A-HA/Rps7B-GST and Rpl16A-GST/Rpl16B-HA pairs were equally incorporated into ribosomes from quiescent and post stimulus cells (Figures S7B and S8B). Next, co-sedimentation analysis was performed across sucrose gradients using extracts from quiescent or 60 min fresh media stimulated cells (Figures S7C and S8C). Rps7A-HA/Rps7B-GST pair principally accumulates in monosome fractions during quiescence, while after nutrient stimulus Rps7A-HA mainly associated with monosomes and Rps7B-GST with polysomes (Figures 3 and S7C). In contrast, Rpl16A-GST and Rpl16B-HA accumulate in monosome fractions during quiescence, and both RP paralogs cofractionate with

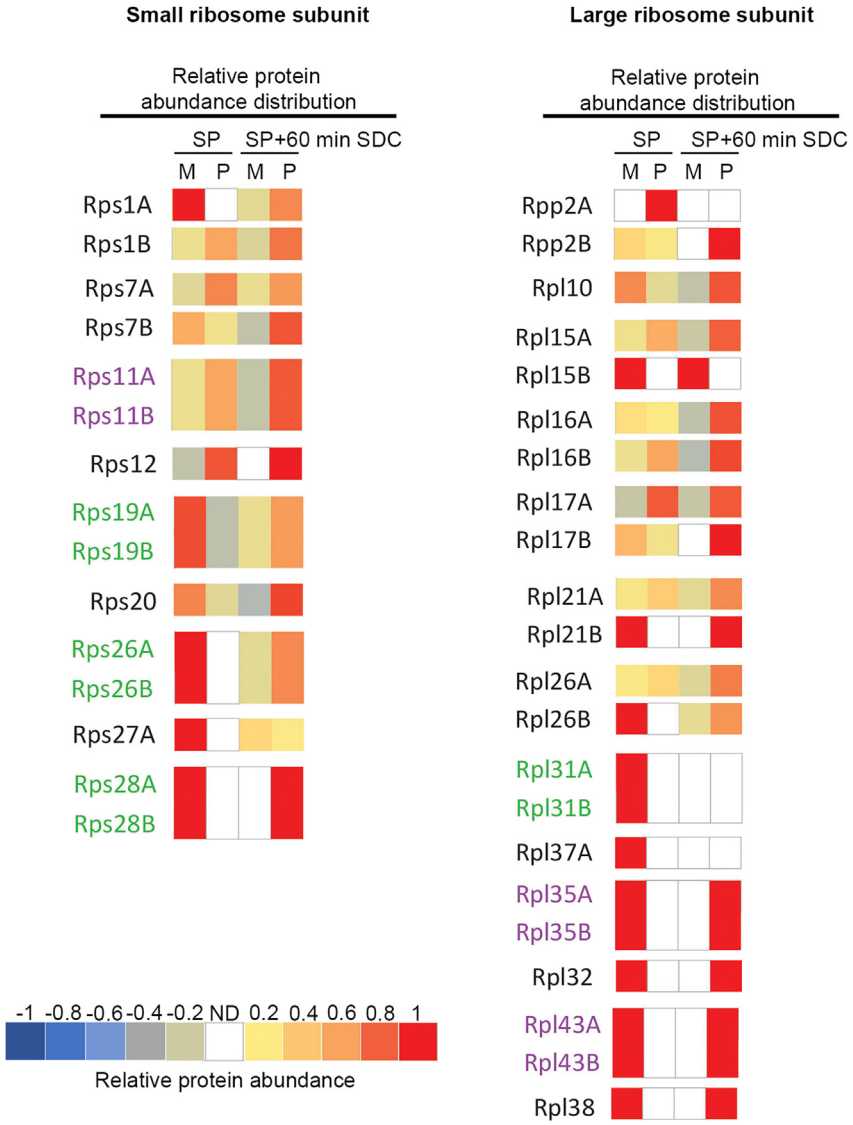

Figure 3. Analysis of the composition of core ribosomal proteins

The relative abundance distribution of the ribosomal proteins of the large and small subunit of the ribosome in monosomal (M) or polysomal (P) fractions. The distribution of different ribosomal proteins in monosomal (M), or polysomal fractions (P) is shown. The emPAI data obtained by nanoLC-MS/MS from stationary phase (SP) or after 60 min of fresh medium stimulus (SP + SDC 60 min) riboproteome were used to calculate the relative protein abundance distribution. Heat maps indicate the distribution of relative abundance between the fractions M and P in each condition. The color scale is indicated, ND = not detected. Relative abundance distribution less than 0.8 was not considered. Ribosomal protein paralogs with 100% identity (violet) and those for which it was not possible to distinguish between paralog pairs (green).

polysomes after stimulus (Figures 3 and S8C). To assess whether ribosomes containing both RP paralogs are present on single mRNAs, a pull-down assay was performed from polysome fractions. The pair of paralogs Rpl16 were chosen since this protein is preferentially located at the solvent-accessible face of ribosomes.[62] Rpl16A-GST purified from nutrient stimulated quiescent cells co-purified with Rpl16B-HA, therefore ribosomes containing Rp116A co-exist on mRNAs with ribosomes containing Rp116B. The results indicates that polysomes contain a mixed paralog population (Figure S8E).

The relative accumulation pattern of RPs encoded by single-copy genes, RP paralogs with 100% identity and RPs paralogs that were indistinguishable from the mass spectrometry analysis (violet and green labeled respectively) was also analyzed (Figure 3). The distribution of a great number of RPs (37) is similar in monosomes and polysomes from quiescence and post-stimulus cells (Table S1). However, some single-gene encoded RPs show differential fractionation. For example, Rpl10, Rpl32, Rpl38 and Rps20 show an enrichment in the polysome fraction following the nutrient stimulus, while Rps12 is exclusively associated with polysome fraction from cells of both analyzed conditions.

Table 1. Summary of relative abundance distribution of RP in ribosomes from quiescent exit cells

	Fraction	
Condition	Monosome	Polysome
SP	Rpl15B^{M} **Rpl32; Rpl43 A/B; Rpl38; Rpl35 A/B; Rpl21B; Rps28 A/B** *Rpl26B; Rpl31 A/B; Rpl37A; Rps1A; Rps26 A/B; Rps27A; Rps19 A/B*	Rps12^{P}; Rpl17A^{P} Rpp2A
SP + 60 min SDC	Rpl15B^{M}	Rps12^{P}; Rpl17A^{P} **Rpl32; Rpl43 A/B; Rpl38** **Rpl35 A/B; Rpl21B; Rps28 A/B** *Rpp2B; Rpl16B and Rpl16A* *Rps7B; Rpl17B; Rpl10; Rps20* *Rps11 A/B*

^{M} and ^{P}: RPs enriched in monosomes or polysomes in both conditions. RPs that change their abundance according to growth conditions are labeled in bold. RPs that show a specific enrichment according to fraction or growth condition are indicated in italics. The specific RP paralog is underlined. SP: Stationary Phase; SP+60 min SDC: stationary phase cells after stimulation with fresh medium for 60 min.

In summary, our results indicates that the RP composition of monosomes and polysomes changes during the translation reactivation that occurs when cells exit quiescence.

Characterization of proteins that co-fractionate with ribosomes

The proteomic analysis of the ribosomes also identified 444 proteins that co-fractionated with the ribosomal proteins. These cofractionating proteins were reclassified according to their functional gene ontology: ribosome biogenesis, translation, proteasome, protein folding, carbon metabolism, ribosome-associated proteins, and miscellanea (Figure 4A). The relative distribution of proteins from different categories was assessed in the free, monosome, and polysome fractions for each of the growth conditions (Table S1). Figure 4B shows the heat maps corresponding to representative proteins from each group. Protein distribution was confirmed using Western blotting from sucrose gradient fractions (Figure S4B).

We identified 15 of the 33 subunits of the 26S proteasome (Table S1; Figure 4B) co-fractionating with the monosomes fractions both pre- and post-stimulus suggesting that the proteasome almost exclusively co-fractionates with the monosome (Figures 4B and S3C). The protein Tma17, which was detected exclusively in the monosome fraction, has been described as a proteasome assembly factor associated with 40S and 60S subunits.[63,64]

It has been described that proteasome assembly involves ribosome pausing and co-translational assembly of Rpt1-Rpt2.[65] However, no bias in the peptide distribution across the Rpt1 primary sequence was observed suggesting that fully translated Rpt1 protein co-fractionates with the monosome.

The interaction between the proteasome and the 80S ribosome has been linked to ribosome associated protein quality control (RQC) mechanisms that survey nascent peptide degradation[66] and/or ribophagy processes.[67] However, neither the monosome nor polysome fractions of quiescent cells contained RQC components. This result agrees with the observation that ribosome pausing overcomes the RQC pathway in aging yeast cells, compromising co-translational proteostasis.[48]

The heterodimers Egd1/Egd2 (polypeptide-associated complex, NAC) as well as Ssz1/Zuo1 (ribosome-associated complex, RAC) co-fractionate with both monosomes and polysomes during stationary phase. Also, subunits of the TRiC complex co-fractionate with monosomes from stimulated stationary phase cells presumably to favor the folding of newly synthesized proteins.[21,68] Other factors and proteins with chaperone activity that assist protein folding, such as Hsp26, Sgt2 and Hsp60 (partially) were enriched in the monosome fraction; whereas Hsp31 was partially enriched in polysome fractions from quiescent cells suggesting that a small number of particular chaperones cooperates with ribosomes to maintain protein folding in dormant cells.

These results suggest that, depending on the nutritional condition, both monosomes and polysomes interact with ribosome-associated protein complexes involved in the regulation of nascent peptides to favor co-translational protein folding, assembly, and ribosomal quality control.

Stm1 was detected in monosomes fractions from quiescent cells and in polysome fractions after stimulation with fresh media (Figure 4B). The role of Stm1 might relate to ribosome preservation during quiescence.[69] Its presence could suggest that a population of Stm1-containing 80S particles would be free of mRNA in quiescent cells.

We identified an enrichment of enzymes that protect from oxidative stress such as Trx1 and Grx2. The association of these enzymes could provide a protective function of ribosome particle from oxidative stress which affects translation.[70]

Overall, our analysis suggests that monosomal and polysomal fractions modify the associated protein pattern according to growth conditions. The enrichment of proteins controlling different processes may functionally interconnect the ribosome with various cellular processes. Further work is required to characterize the functions of ribosome-associated proteins in translation regulation during quiescence exit.

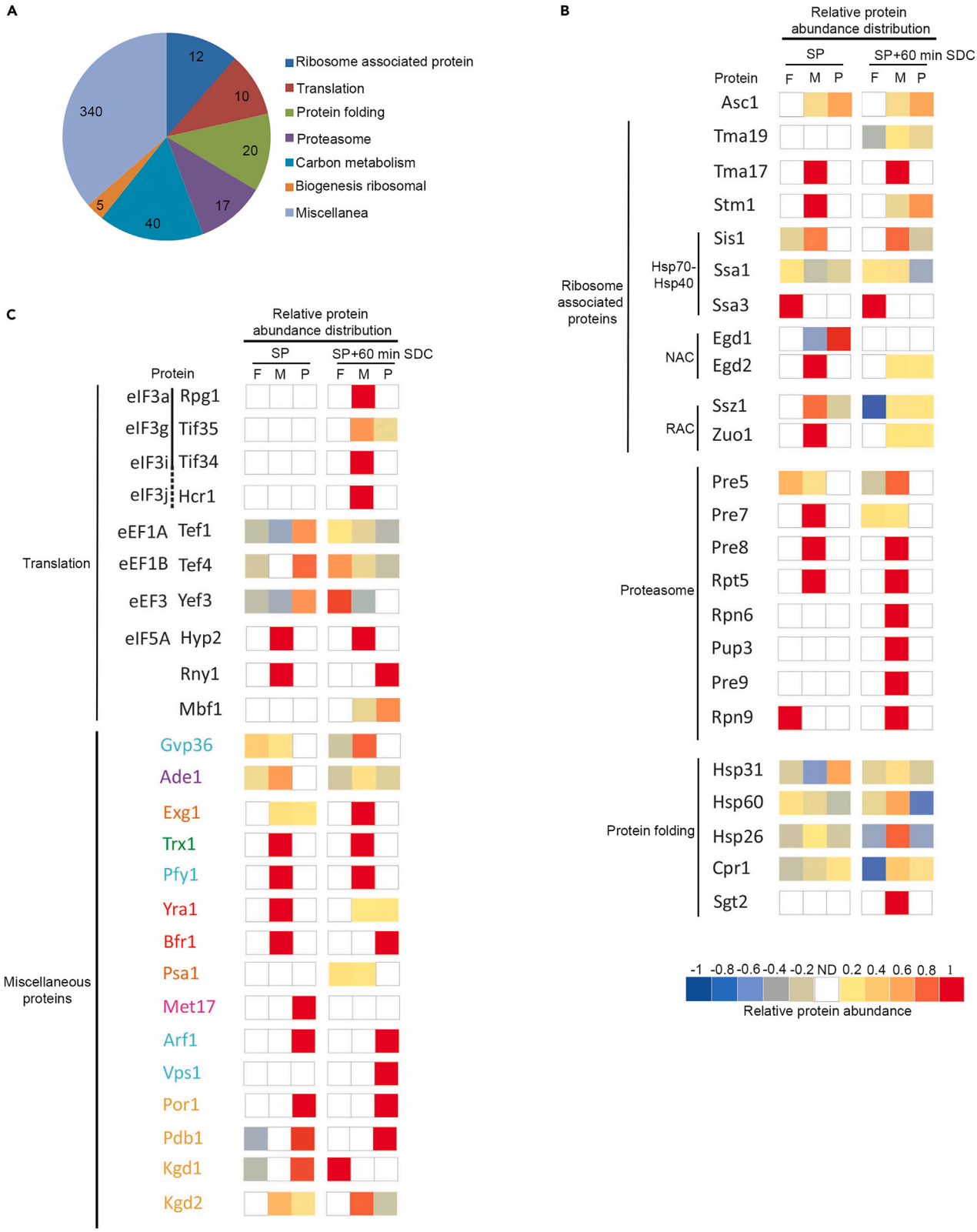
A
12
10
20
17
40
5
340
Ribosome associated protein
Translation
Protein folding
Proteasome
Carbon metabolism
Biogenesis ribosomal
Miscellanea
B
Relative protein abundance distribution
SP
SP+60 min SDC
Protein
F M P F M P
Asc1
Tma19
Tma17
Stm1
Sis1
Ssa1
Ssa3
Egd1
Egd2
Ssz1
Zuo1
Pre5
Pre7
Pre8
Rpt5
Rpn6
Pup3
Pre9
Rpn9
Hsp31
Hsp60
Hsp26
Cpr1
Sgt2
Ribosome associated proteins
Hsp70-Hsp40
NAC
RAC
Proteasome
Protein folding
-1 -0.8 -0.6 -0.4 -0.2 ND 0.2 0.4 0.6 0.8 1
Relative protein abundance
C
Relative protein abundance distribution
SP
SP+60 min SDC
Protein
F M P F M P
eIF3a Rpg1
eIF3g Tif35
eIF3i Tif34
eIF3j Hcr1
eEF1A Tef1
eEF1B Tef4
eEF3 Yef3
eIF5A Hyp2
Rny1
Mbf1
Gvp36
Ade1
Exg1
Trx1
Pfy1
Yra1
Bfr1
Psa1
Met17
Arf1
Vps1
Por1
Pdb1
Kgd1
Kgd2
Translation
Miscellaneous proteins

Figure 4. Characterization of co-fractionated proteins with the core ribosomal proteins

(A) The pie chart shows the number of unique proteins identified in this study, classified by Gene Ontology.

(B and C) The relative abundance distribution of different proteins in free (F), monosomal (M), or polysomal fractions (P) is shown. The emPAI data obtained by nanoLC-MS/MS from stationary phase (SP) or after 60 min of fresh medium stimulus (SP + SDC 60 min) riboproteome were used to calculate the relative protein abundance distribution. Heat maps indicate the distribution of relative abundance between the fractions F, M, and P in each condition. The color scale is indicated, ND = not detected. Relative abundance distribution less than 0.8 was not considered. Representative proteins from proteasome, protein folding, translation, and miscellaneous groups are shown (Table S1, Protein abundance F, M, P). Representative proteins of each category are shown, nucleotide biosynthetic process purine (violet), amino acid biosynthesis (pink), mRNA binding (red), oxidative stress (green), cellular transport and large membranous structures (light blue), and mitochondria (brown).

Role of ribosomal proteins on translational activity from quiescent exist cells

Based on the results above we conclude that RP stoichiometry changes during the translational activation of quiescent cells (Table 1). Next, we evaluated the role of individual RPs, investigating cell growth and global translational activity in cells where an RP gene is deleted (Figure 5).

From the RPs encoded by a unique gene, Rps12, Rpl38, Rpp2A, and Rpp2B were chosen since *RPS20*, *RPL10*, and *RPL32* are essential genes (Table S3). For those RP paralogs with high protein sequence homology (97–99%), such as Rpl15 A/B, Rpl17 A/B, and Rpl21 A/B, deletion of one of the genes can cause inviability.[7,19,71] Therefore, we chose the Rps7A/Rps7B, Rpl16A/Rpl16B and Rpl37A/Rpl37B paralogs, which exhibit the most diverged amino acid sequences and individual paralog deletion is viable (Table S3).

First, we evaluated the consequences of the deletion of single RP paralog genes or deletion of non-paralog RP genes on growth fitness during quiescence exit (Figures 5A and 5B). Figures 5A and S9A show that all of the RP gene deletion strains reach the same OD_{600nm} after 72 h of growth and most of the strains exhibit similar cellular viability both in the stationary phase or after 180 min of nutrient stimulus. However, the pairs *RPP2A/B* and *RPS7A/B* show differences in the duration of lag phase; deletion of *RPP2B* or *RPS7A* delayed cellular growth during exit from quiescence. In contrast, the non-paralog *RPL38* deletion partially reduces the lag phase length during the quiescence exit (Figure 5B). The results suggest RP-specific effects directing the efficiency of outgrowth from quiescence.

Next, the role of RPs on the global translational activation of nutrient stimulated quiescent cells was evaluated. Puromycin incorporation and Renilla luciferase translation reporter assays were performed (Figures 5C and 5D). Compared to wild-type cells, yeast with *RPL38* deletion show a decrease in translational activity. These findings suggest that Rpl38 enrichment into the polysome (Figure 3) positively contributes to translation activity and accurate phase lag duration. As previously described there may be a fitness trade-off between phase lag duration, environmental conditions and cell metabolism.[72]

The single deletions of *RPS7A*/*RPS7B*, *RPL16A*/*RPL16B*, and *RPL37A*/*RPL37* paralog genes affect translational activity during quiescence exit. It was described that the deletion of RP genes impacts rRNA biogenesis.[19,71] To verify that the deletions of RPs genes does not affect rRNA biogenesis the 25S/18S rRNA ratio in the mutant strains used in this study was assessed. Yeast cells from the stationary phase and from 180 min after stimulation with fresh medium (Figure S9D) show no change in the levels of rRNA. Therefore, the changes observed in the RP gene-deleted mutant strains both in growth fitness and global translation are not a consequence of an imbalance in major and minor ribosome subunits.

From the Rps7A/B pairs, the paralog Rps7B is the most heavily expressed both in stationary phase and after nutrient stimulus (Figure S5B), which differs from expression in exponential phase cells.[71] Both paralogs show a distinct distribution in monosome and polysome fractions from stationary cells after nutrient stimulus. Rps7B is associated with polysomes whereas Rps7A remains associated with monosomes fractions (Figures 3 and S7C). The low levels of Rps7A in the polysome fraction suggest that translating ribosomes could be composed of one of the two Rps7 paralogs. Figures 5C and 5D show that *RPS7A* deletion significantly reduced global translation activity in comparison to *RPS7B* deletion. Therefore, these results suggest that both Rps7 paralogs carry out different roles in translation. Previous work has suggested that the deletion of either gene affects the expression of the other in exponentially growing cells.[71] However, there is no evidence that the *RPS7A* or *RPS7B* gene deletions alter the expression of the paralogous gene in quiescent cells. Therefore, it is difficult distinguish whether the changes in global translation activity upon *RPS7* gene deletion are a consequence of reduced overall gene dose or paralog specific requirements.

The pair of paralogs Rpl16 A/B exhibit different behavior. Analysis of RP expression from strains expressing chromosomally tagged Rpl16A-ZZ or Rpl16B-ZZ shown that Rpl16B is the main paralog across most conditions: in stationary phase, after nutrient stimulus (Figure S8D) and in the exponential growth phase (Figure S8D).[7] Both Rpl16 paralogs show similar distribution in polysomes upon fresh medium addition to stationary phase cells (Figures 3 and S8C). Pull-down assays of Rpl16A-GST suggest that a mixed population of Rpl16A and Rpl16B ribosomes exist on individual mRNAs (Figure S8E). The level of the Rpl16B paralog is generally higher than Rpl16A thus some polysomes containing only the Rpl16B paralog might be expected. A strain carrying the *RPL16B* deletion shows lower translational activity than a strain lacking the *RPL16A* gene suggesting a different role of these paralogs in translation (Figures 5C and 5D). Finally, another example is the Rpl37 A/B pair, from which only the Rpl37A paralog is detected by MS. This protein associates exclusively with the monosome fraction in quiescent cells (Figure 3). *RPL37A* deletion decreases the global translational activity while *RPL7B* deletion has no effect (Figures 5B and 5C). Again, this result suggests a different role of each paralog in translation. For Rpl16 A/B and Rpl37 A/B it cannot be distinguished if the changes in global translation activity upon RP gene deletion are a consequence of gene dose or gene type requirements.

Altogether, differential expression of RPs and their association with ribosomes might give rise to the formation of heterogeneous ribosomes allowing a diversity in translation functionality during quiescence exit.

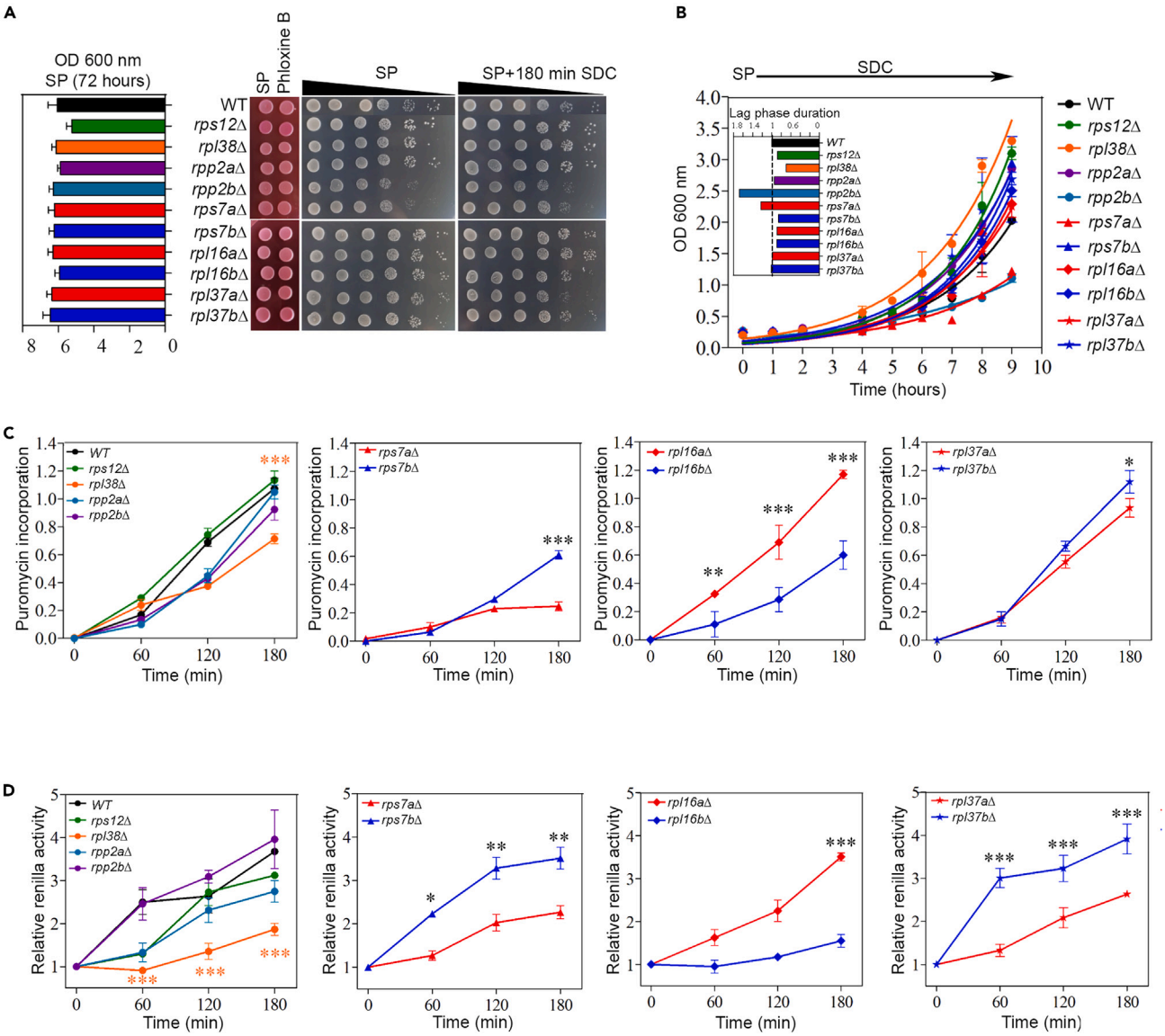

Figure 5. Deletion of specific RPs alters translational activity during quiescent exit

(A) Maximum cell density measured at A_{600}nm after 72 h growth (n = 6 biological replicates) and cell viability of quiescent cells evaluated by spot assay and phloxine B incorporation. Spotted plates were photographed after 24 h and 48 h (Figure S9A).

(B) Cell growth of stationary phase cells stimulated with fresh SDC media (n = 3 biological replicates). The inset shows the lag phase length. Logistic population growth was adjusted using Graphpad Prism 8.

(C) Global translational activity was measured by puromycin incorporation during quiescence exit. Neosynthesized proteins were labeled with puromycin and analyzed by Western blot and quantified by densitometry (***p < 0.001; **p < 0.01; *p < 0,05, n = 3 biological replicates, Figure S10).

(D) Translation activity was evaluated with Renilla luciferase reporter (n = 3 biological replicates). For the time course data, a two-way ANOVA with Bonferroni's multiple comparison test was used to assess differences between time points (***p < 0.001; **p < 0.01; *p < 0,05). Control experiments shows that the Renilla mRNA level does not differ between strains (Figure S7B).

DISCUSSION

Translational activation during quiescence exit

During quiescence in *S. cerevisiae* the rate of protein translation is severely reduced by coordinated events such as the downregulation of both RP and translation factors, and the global inhibition of translation initiation. The remaining translational capacity is dedicated to the synthesis of proteins necessary for cell viability during quiescence.[73] Our results show that the RPs and rRNA levels remain similar in both quiescent cells and cells that are followed by 60 min of rich media stimulation. Following the 60 min stimulation, the increase in polysomes suggests that global translation is reactivated. For two genes, *ENO2* and *PAB1*, we observed a reduction of total mRNA, polysome-associated mRNA,

and steady state protein quantity during the stationary phase with the levels being restored upon refeeding. For another gene, *NCE102*, we observed a large increase in mRNA levels in quiescent cells that appears to drive a corresponding increment in protein levels, although the proportion of mRNA associated with polysomes was reduced. Nce102 protein level increase at the beginning of the diauxic shift and is maintained during the stationary phase.[51] Nce102 regulates eisosome formation, which plays important roles in regulating nutrient uptake to prepare cells to enter the later stages of growth and the stationary phase.[74]

The behavior of another glycolytic gene (*PDC1*) is quite different. The levels of polysome-associated *PDC1* mRNA remain high during the stationary phase. The decrease in Pdc1 protein abundance could be a consequence of low levels of mRNA. Indeed, IRES elements promote mRNA translation during quiescence.[75] However, there is no IRES described in the *PDC1* mRNA sequence. Alternatively, even given the compact nature of the *PDC1* 5′UTR, it is still possible that *cis*-acting elements in the 5′UTR of *PDC1* mRNA could be necessary to improve its translation efficiency; however, the precise mechanism involved in this mRNA translation remains to be determined.

These results showed a positive correlation between protein expression and mRNA levels during both quiescence and after translational reactivation following stimulation with fresh media. These findings are in agreement with studies analyzing genome-wide mRNA and protein expression level in yeast cells in response to different stresses. These experiments demonstrate that a good proportion of changes to protein levels occur as a consequence of alterations in both mRNA levels and the degree of mRNA association with polysomes.[76–78]

Different ribosome subpopulations in both monosomes and polysomes are sensitive to nutrient stimulation

Following a nanoLC-MS/MS strategy, we observed a dynamic change in ribosome composition during quiescence exit. The relative abundance of many RPs varied between monosomes and polysomes depending on the nutrient stimulus. For instance, RPs enriched in monosomes during quiescence were re-distributed toward polysomes upon translational activation after the addition of fresh media. However, some RPs exhibited enrichment in monosomes from dormant cells, whilst others were more prevalent in polysome fractions following stimulation (Table 1). Most strikingly perhaps is the finding, across several RP paralogous pairs, of only one paralog associated with monosomes or polysomes under different growth conditions. The RP composition of monosomes and polysomes in both quiescent and post stimulus conditions differs from that of glucose grown cells.[29,31] This observation suggests that quiescent exit cells have a specific RP repertoire. Ribosome differences between monosomal and polysomal ribosomes may indicate distinct translational activity.

As previously mentioned, the RP composition of yeast grown on glucose differs from that of polysomes from stimulated quiescent cells, Slavov et al.[29] reported that RP stoichiometry correlates with growth rate. However, a similar analysis revealed no correlation between cellular fitness[79] and the RP composition of polysomes characterized in our work. We hypothesize that ribosome composition is an intermediary step in cell adaptation to changing environments during the quiescence-growth transition.

In *S. cerevisiae*, 59 of the 78 RP genes are retained as two genomic copies.[80] We observed several RP paralogs that are associated with the same fraction under both growth conditions. Since it has been described that two RPs paralogs cannot assemble into the same ribosome particle simultaneously, the detection of the two paralog proteins in the same fraction (monosome or polysome) indicates that there are subpopulations of ribosomal particles differing in composition at the RP paralog level. Regardless of the fact that RP paralogs have nearly identical amino acid sequences, studies have demonstrated paralog-specific functions.[6,8,28] Indeed, our results show that several RP paralogs found in quiescent cells play a specific function in translation as a consequence of gene dose or gene type requirements.

The eukaryotic ribosome assembly pathway involves more than 200 factors and spans various subcellular compartments.[3] Following the completion of maturation, the 40S and 60S ribosomal subunits are held together either on the mRNA during translation or via specific proteins when free.[81] The crystal structure of the 80S ribosome from glucose-starved yeast shows that Stm1 occupies part of the mRNA channel. The presence of Stm1 stabilizes 80S by clamping the 40S and 60S subunits and inhibits translation by excluding mRNA binding.[81] Previous results show that the ribosome-associated protein Stm1 prevents ribophagy during quiescence and thus may promote ribosome availability for translation once nutrients become available.[69] We have shown in this work that Stm1 predominantly cofractionates with monosomes during quiescence, indicating the existence of a subpopulation of 80S ribosomes bound to Stm1. The preservation of 80S during quiescence can be useful for ribosome recycling when nutrients trigger translational activation but no new ribosomes are already synthesized (at least for the first 60 min after stimulus). Accordingly, several RP monosomes from quiescent cells move to polysomes after stimulation with fresh media.

Substantial evidence from various biological systems suggests that ribosome remodeling or repair can occur directly on ribosomes, for example, in response to ribophagy in the bacterial ribosome,[82] hepatocyte ribosome composition remodels in response to an altered diet,[83] and in neuronal ribosomes following oxidative stress.[84] In yeast, translation activation after glucose refeeding to glucose-starved exponential yeast cells shows a ribosome shifting from 80S back to polysomes.[85]

Ribosomal biogenesis decreases during quiescence.[73] Quiescent cells show an increase in ribosomal protein levels via *de novo* synthesis after 2 h of stimulation[86] and mutants with defects in ribosomal biogenesis fail to resume growth from quiescence.[87] Our analysis shows that the expression level of most RPs from quiescent cells remains constant after 60 min following nutrient stimulus or refeeding and we posit that these RPs detected in pre- and post-stimulated quiescent cells are part of ribosome particles, since we did not detect them in sub-ribosomal gradient fractions. In addition, it could also be that RPs that fail to assemble into ribosomes are rapidly ubiquitinated and degraded in the nucleus in a proteasome-dependent manner as previously described.[88] Nevertheless, since the populations of ribosome subunits after 60 min of stimulation have different protein composition to those seen during quiescence, it appears that another process is responsible for the diversity of ribosomes raising the possibility that RPs could be exchanged using *de novo* synthesized RPs produced during quiescence exit. On the other hand, 80S ribosomes from quiescent cells could be recycled to polysomes once translational activity is induced. Further research is required to explore the mechanism underlying the remodeling of RP content during the first steps of the quiescence-growth transition, which results in ribosome heterogeneity.

The ribosomal fractions from quiescence exit contain proteins that belong to various functional groups such as translation, protein folding, metabolism, and response to oxidative stress, among others. These non-ribosomal proteins could be defined as ribosome-associated proteins. Proteasome components and Tma17 were associated with monosomes regardless of the stimulus. Proteasome-ribosome interaction could imply changes in the control of the nascent peptide and/or in the homeostasis of ribosomes.[89] It has been reported that Tma17 interacts with the ribosome and proteasome, suggesting that Tma17 could be involved in the proteasome-80S crosstalk.[63,64]

In this study, a subunit of the RAC complex, Zuo1, was identified in the monosomal fraction of quiescent cells. This protein interacts with both ribosome subunits and has a direct role in translational fidelity.[90] It has been described that monosome 80S particles can actively translate mRNAs encoding low-abundance regulatory proteins in yeast[91] and neurons.[92] Indeed, our data shows the presence of translational elongation factors, nascent peptide chaperones (e.g., RAC, NAC), and proteasome proteins among others associated with the monosome. However, these same factors might also be present where subpopulations of 80S stalled ribosomes accumulate.[48,93]

The polysomes from quiescent cells are enriched in chaperone proteins and translation elongation factors suggesting actively translating ribosomes. Furthermore, glycolytic enzymes were detected associated with polysomes and this localization might supply the energy required for translation and/or could direct non-canonical functions for these proteins in translation regulation. For example, mammalian muscle pyruvate kinase has been shown to function as an RNA-binding protein in the translation of mRNA destined for the endoplasmic reticulum.[9]

In yeasts, it has been described that ribosomal particles can present protruded rRNAs acting as scaffolds. Different functional groups of proteins are recruited to these platforms to modify the ribosomal functions.[23] We found that Asc1 exhibited partial presence in polysomes regardless of growth conditions. Asc1 (homologous to mammalian RACK1) is thought to function as a scaffold for non-ribosomal proteins.[94]

In conclusion, we present evidence which indicates that the ribosomes from monosomes or polysomes present different protein composition during quiescence exit. This protein composition is sensitive to nutrient availability. The resulting ribosomal heterogeneity is a consequence of the replacement and the variation of stoichiometry between paralog RPs both in monosome and polysome fractions and also in quiescent and nutrient stimulated cells. This heterogeneity may or may not imply a functional change of specialization of the ribosomes.[95] The role of ribosome populations on mRNA translation selectivity on proteome adjustment during quiescence-growth transition deserves further investigation.

Limitation of the study

Using a nanoLC-MS/MS strategy, this study provides a comprehensive characterization of the dynamic of riboproteome in *S. cerevisiae*. Further functional experiments to characterise the role of the diversity ribosome during quiescence exit would strengthen the results of this study. Proteomic approaches present certain limitations: It is well known that MS data acquisition results in a significant percentage of missing values in proteomics datasets because of the semi-stochasticity of ionization, fragmentation, and detection of peptides and fragments. MS protein identification is a probabilistic technique, and even though we conducted validation studies, only a small number of targets were validated in terms of the mass spectrometry dataset.

STAR★METHODS

Detailed methods are provided in the online version of this paper and include the following:

- KEY RESOURCES TABLE
- RESOURCE AVAILABILITY
  - Lead contact
  - Materials availability
  - Data and code availability
- EXPERIMENTAL MODEL AND STUDY PARTICIPANT DETAILS
  - Yeast strains
- METHOD DETAILS
  - Crude extract preparation
  - Serial dilution assay
  - Puromycin incorporation assay
  - Western blot analysis
  - Protein half-life analysis
  - Strains construction
  - Sucrose cushions analysis
  - Ribosome co-sedimentation analysis
  - Purification of ribosomes containing Rpl16A-GST
  - RT-qPCR
  - Renilla luciferase assay
  - Sample preparation and mass spectrometry
  - Analysis of mass spectrometry spectra
  - String analysis
- QUANTIFICATION AND STATISTICAL ANALYSIS

SUPPLEMENTAL INFORMATION

Supplemental information can be found online at https://doi.org/10.1016/j.isci.2023.108727.

ACKNOWLEDGMENTS

We are grateful to M. Pool (The University of Manchester) for the kind gift of anti-Rps3 and anti-Rpl35 antibodies, M. Monte (University of Buenos Aires) for the kind gift of anti-HA antibody, A. Gerber for the kind gift of Rpl16A-ZZ and Rpl16B-ZZ strains and K. Karbstein for the kind gift of pKK3700 plasmid. Silvia Rossi was supported by grants from Agencia Nacional de Promoción Científica y Tecnológica [PICT 2014-2937], from the University of Buenos Aires [UBACYT2016. 20020150100035BA] and from Consejo Nacional de Investigaciones Científicas y Técnicas [PIP 112-20110100826]. Clara A. Solari had a CONICET doctoral fellowship and was awarded a Journal of Cell Science traveling fellowship. María Clara Ortolá Martínez has a CONICET doctoral fellowship. Fabián Morales-Polanco was supported by a CONICYT Becas Chile doctoral studentship (72140307). Paula Portela was supported by a grant from Agencia Nacional de Promoción Cientifica y Tecnologica [PICT 2017-2240] and [PICT2021-4843]. Mark P. Ashe was supported by the Biotechnology and Biological Sciences Research Council grant [BB/K005979/1]. Silvia Rossi, María Pia Valacco, Silvia Moreno and Paula Portela are researchers from CONICET.

AUTHOR CONTRIBUTIONS

Conceptualization, C.A.S., P.P., and G.C.; methodology, C.A.S., C.B., M.P.V., and P.P.; formal analysis, G.C., M.P.V., and S.M.; investigation, C.A.S., M.C.O.M., J.M.F., C.B., and P.P.; resources, S.M., S.R., P.P., and M.P.A.; writing – original draft and visualization, C.A.S. and P.P.; writing – review & editing: all authors; supervision, P.P.; funding acquisition, P.P., S.R., and M.P.A.

DECLARATION OF INTERESTS

The authors declare no competing interests.

INCLUSION AND DIVERSITY

We support inclusive, diverse, and equitable conduct of research.

Received: February 2, 2023
Revised: August 15, 2023
Accepted: December 11, 2023
Published: December 14, 2023

REFERENCES

1. Shu, X.E., Swanda, R.V., and Qian, S.B. (2020). Nutrient Control of mRNA Translation. Annu. Rev. Nutr. *40*, 51–75.
2. Genuth, N.R., and Barna, M. (2018). The Discovery of Ribosome Heterogeneity and Its Implications for Gene Regulation and Organismal Life. Mol. Cell *71*, 364–374.
3. Peña, C., Hurt, E., and Panse, V.G. (2017). Eukaryotic ribosome assembly, transport and quality control. Nat. Struct. Mol. Biol. *24*, 689–699.
4. Emmott, E., Jovanovic, M., and Slavov, N. (2019). Ribosome Stoichiometry: From Form to Function. Trends Biochem. Sci. *44*, 95–109.
5. Whittle, C.A., and Krochko, J.E. (2009). Transcript profiling provides evidence of functional divergence and expression networks among ribosomal protein gene paralogs in Brassica napus. Plant Cell *21*, 2203–2219.
6. Segev, N., and Gerst, J.E. (2018). Specialized ribosomes and specific ribosomal protein paralogs control translation of mitochondrial proteins. J. Cell Biol. *217*, 117–126.
7. Ghulam, M.M., Catala, M., and Abou Elela, S. (2020). Differential expression of duplicated ribosomal protein genes modifies ribosome composition in response to stress. Nucleic Acids Res. *48*, 1954–1968.
8. Komili, S., Farny, N.G., Roth, F.P., and Silver, P.A. (2007). Functional specificity among ribosomal proteins regulates gene expression. Cell *131*, 557–571.
9. Simsek, D., Tiu, G.C., Flynn, R.A., Byeon, G.W., Leppek, K., Xu, A.F., Chang, H.Y., and Barna, M. (2017). The Mammalian Ribo-interactome Reveals Ribosome Functional Diversity and Heterogeneity. Cell *169*, 1051–1065.e18.
10. Ruvinsky, I., Sharon, N., Lerer, T., Cohen, H., Stolovich-Rain, M., Nir, T., Dor, Y., Zisman, P., and Meyuhas, O. (2005). Ribosomal protein S6 phosphorylation is a determinant of cell size and glucose homeostasis. Genes Dev. *19*, 2199–2211.
11. Ceci, M., Gaviraghi, C., Gorrini, C., Sala, L.A., Offenhäuser, N., Marchisio, P.C., and Biffo, S. (2003). Release of eIF6 (p27BBP) from the 60S subunit allows 80S ribosome assembly. Nature *426*, 579–584.
12. Gunderson, J.H., Sogin, M.L., Wollett, G., Hollingdale, M., de la Cruz, V.F., Waters, A.P., and McCutchan, T.F. (1987). Structurally distinct, stage-specific ribosomes occur in Plasmodium. Science *238*, 933–937.
13. Parks, M.M., Kurylo, C.M., Dass, R.A., Bojmar, L., Lyden, D., Vincent, C.T., and Blanchard, S.C. (2018). Variant ribosomal RNA alleles are conserved and exhibit tissue-specific expression. Sci. Adv. *4*, eaao0665.
14. Sloan, K.E., Warda, A.S., Sharma, S., Entian, K.D., Lafontaine, D.L.J., and Bohnsack, M.T. (2017). Tuning the ribosome: The influence of rRNA modification on eukaryotic ribosome biogenesis and function. RNA Biol. *14*, 1138–1152.
15. Lilleorg, S., Reier, K., Pulk, A., Liiv, A., Tammsalu, T., Peil, L., Cate, J.H.D., and Remme, J. (2019). Bacterial ribosome heterogeneity: Changes in ribosomal protein composition during transition into stationary growth phase. Biochimie *156*, 169–180.
16. Mageeney, C.M., and Ware, V.C. (2019). Specialized eRpL22 paralogue-specific ribosomes regulate specific mRNA translation in spermatogenesis in Drosophila melanogaster. Mol. Biol. Cell *30*, 2240–2253.
17. Anderson, S.J., Lauritsen, J.P.H., Hartman, M.G., Foushee, A.M.D., Lefebvre, J.M., Shinton, S.A., Gerhardt, B., Hardy, R.R., Oravecz, T., and Wiest, D.L. (2007). Ablation of ribosomal protein L22 selectively impairs alphabeta T cell development by activation of a p53-dependent checkpoint. Immunity *26*, 759–772.
18. Lopes, A.M., Miguel, R.N., Sargent, C.A., Ellis, P.J., Amorim, A., and Affara, N.A. (2010). The human RPS4 paralogue on Yq11.223 encodes a structurally conserved ribosomal protein and is preferentially expressed during spermatogenesis. BMC Mol. Biol. *11*, 33.
19. Parenteau, J., Lavoie, M., Catala, M., Malik-Ghulam, M., Gagnon, J., and Abou Elela, S.

(2015). Preservation of Gene Duplication Increases the Regulatory Spectrum of Ribosomal Protein Genes and Enhances Growth under Stress. Cell Rep. *13*, 2516–2526.
20. Deuerling, E., Gamerdinger, M., and Kreft, S.G. (2019). Chaperone Interactions at the Ribosome. Cold Spring Harb. Perspect. Biol. *11*, a033977.
21. Morales-Polanco, F., Lee, J.H., Barbosa, N.M., and Frydman, J. (2022). Cotranslational Mechanisms of Protein Biogenesis and Complex Assembly in Eukaryotes. Annu. Rev. Biomed. Data Sci. *5*, 67–94.
22. Anger, A.M., Armache, J.P., Berninghausen, O., Habeck, M., Subklewe, M., Wilson, D.N., and Beckmann, R. (2013). Structures of the human and Drosophila 80S ribosome. Nature *497*, 80–85.
23. Fujii, K., Susanto, T.T., Saurabh, S., and Barna, M. (2018). Decoding the Function of Expansion Segments in Ribosomes. Mol. Cell *72*, 1013–1020.e6.
24. Schmitt, K., Kraft, A.A., and Valerius, O. (2021). A Multi-Perspective Proximity View on the Dynamic Head Region of the Ribosomal 40S Subunit. Int. J. Mol. Sci. *22*, 11653.
25. Boria, I., Garelli, E., Gazda, H.T., Aspesi, A., Quarello, P., Pavesi, E., Ferrante, D., Meerpohl, J.J., Kartal, M., Da Costa, L., et al. (2010). The ribosomal basis of Diamond-Blackfan Anemia: mutation and database update. Hum. Mutat. *31*, 1269–1279.
26. Aspesi, A., and Ellis, S.R. (2019). Rare ribosomopathies: insights into mechanisms of cancer. Nat. Rev. Cancer *19*, 228–238.
27. Dauwerse, J.G., Dixon, J., Seland, S., Ruivenkamp, C.A.L., van Haeringen, A., Hoefsloot, L.H., Peters, D.J.M., Boers, A.C.d., Daumer-Haas, C., Maiwald, R., et al. (2011). Mutations in genes encoding subunits of RNA polymerases I and III cause Treacher Collins syndrome. Nat. Genet. *43*, 20–22.
28. Samir, P., Browne, C.M., Rahul, Sun, M., Shen, B., Li, W., Frank, J., and Link, A.J. (2018). Identification of Changing Ribosome Protein Compositions using Mass Spectrometry. Proteomics *18*, e1800217.
29. Slavov, N., Semrau, S., Airoldi, E., Budnik, B., and van Oudenaarden, A. (2015). Differential Stoichiometry among Core Ribosomal Proteins. Cell Rep. *13*, 865–873.
30. Ferretti, M.B., Ghalei, H., Ward, E.A., Potts, E.L., and Karbstein, K. (2017). Rps26 directs mRNA-specific translation by recognition of Kozak sequence elements. Nat. Struct. Mol. Biol. *24*, 700–707.
31. Wang, Y.J., Vaidyanathan, P.P., Rojas-Duran, M.F., Udeshi, N.D., Bartoli, K.M., Carr, S.A., and Gilbert, W.V. (2018). Lso2 is a conserved ribosome-bound protein required for translational recovery in yeast. PLoS Biol. *16*, e2005903.
32. Valcourt, J.R., Lemons, J.M.S., Haley, E.M., Kojima, M., Demuren, O.O., and Coller, H.A. (2012). Staying alive: metabolic adaptations to quiescence. Cell Cycle *11*, 1680–1696.
33. Fuge, E.K., Braun, E.L., and Werner-Washburne, M. (1994). Protein synthesis in long-term stationary-phase cultures of Saccharomyces cerevisiae. J. Bacteriol. *176*, 5802–5813.
34. Tapia, H., and Morano, K.A. (2010). Hsp90 nuclear accumulation in quiescence is linked to chaperone function and spore development in yeast. Mol. Biol. Cell *21*, 63–72.
35. Iwama, R., and Ohsumi, Y. (2019). Analysis of autophagy activated during changes in carbon source availability in yeast cells. J. Biol. Chem. *294*, 5590–5603.
36. Werner-Washburne, M., Braun, E.L., Crawford, M.E., and Peck, V.M. (1996). Stationary phase in Saccharomyces cerevisiae. Mol. Microbiol. *19*, 1159–1166.
37. Berset, C., Trachsel, H., and Altmann, M. (1998). The TOR (target of rapamycin) signal transduction pathway regulates the stability of translation initiation factor eIF4G in the yeast Saccharomyces cerevisiae. Proc. Natl. Acad. Sci. USA *95*, 4264–4269.
38. Tudisca, V., Simpson, C., Castelli, L., Lui, J., Hoyle, N., Moreno, S., Ashe, M., and Portela, P. (2012). PKA isoforms coordinate mRNA fate during nutrient starvation. J. Cell Sci. *125*, 5221–5232.
39. Woodward, K., and Shirokikh, N.E. (2021). Translational control in cell ageing: an update. Biochem. Soc. Trans. *49*, 2853–2869.
40. Sagot, I., and Laporte, D. (2019). The cell biology of quiescent yeast - a diversity of individual scenarios. J. Cell Sci. *132*, jcs213025.
41. Shah, K.H., Zhang, B., Ramachandran, V., and Herman, P.K. (2013). Processing body and stress granule assembly occur by independent and differentially regulated pathways in Saccharomyces cerevisiae. Genetics *193*, 109–123.
42. Barraza, C.E., Solari, C.A., Rinaldi, J., Ojeda, L., Rossi, S., Ashe, M.P., and Portela, P. (2021). A prion-like domain of Tpk2 catalytic subunit of protein kinase A modulates P-body formation in response to stress in budding yeast. Biochim. Biophys. Acta. Mol. Cell Res. *1868*, 118884.
43. Buchan, J.R., Yoon, J.H., and Parker, R. (2011). Stress-specific composition, assembly and kinetics of stress granules in Saccharomyces cerevisiae. J. Cell Sci. *124*, 228–239.
44. Hoyle, N.P., Castelli, L.M., Campbell, S.G., Holmes, L.E.A., and Ashe, M.P. (2007). Stress-dependent relocalization of translationally primed mRNPs to cytoplasmic granules that are kinetically and spatially distinct from P-bodies. J. Cell Biol. *179*, 65–74.
45. Gasch, A.P., Spellman, P.T., Kao, C.M., Carmel-harel, O., Eisen, M.B., Storz, G., Botstein, D., and Brown, P.O. (2000). Genomic expression programs in the response of yeast cells to environmental changes. Mol. Biol. Cell *11*, 4241–4257.
46. Martinez, M.J., Roy, S., Archuletta, A.B., Wentzell, P.D., Anna-Arriola, S.S., Rodriguez, A.L., Aragon, A.D., Quiñones, G.A., Allen, C., and Werner-Washburne, M. (2004). Genomic analysis of stationary-phase and exit in Saccharomyces cerevisiae: gene expression and identification of novel essential genes. Mol. Biol. Cell *15*, 5295–5305.
47. Davidson, G.S., Joe, R.M., Roy, S., Meirelles, O., Allen, C.P., Wilson, M.R., Tapia, P.H., Manzanilla, E.E., Dodson, A.E., Chakraborty, S., et al. (2011). The proteomics of quiescent and nonquiescent cell differentiation in yeast stationary-phase cultures. Mol. Biol. Cell *22*, 988–998.
48. Stein, K.C., Morales-Polanco, F., van der Lienden, J., Rainbolt, T.K., and Frydman, J. (2022). Ageing exacerbates ribosome pausing to disrupt cotranslational proteostasis. Nature *601*, 637–642.
49. Moharir, A., Gay, L., Appadurai, D., Keener, J., and Babst, M. (2018). Eisosomes are metabolically regulated storage compartments for APC-type nutrient transporters. Mol. Biol. Cell *29*, 2113–2127.
50. Murphy, J.P., Stepanova, E., Everley, R.A., Paulo, J.A., and Gygi, S.P. (2015). Comprehensive Temporal Protein Dynamics during the Diauxic Shift in Saccharomyces cerevisiae. Mol. Cell. Proteomics *14*, 2454–2465.
51. Kumar, R., and Srivastava, S. (2016). Quantitative proteomic comparison of stationary/G0 phase cells and tetrads in budding yeast. Sci. Rep. *6*, 32031.
52. Desmyter, L., Verstraelen, J., Dewaele, S., Libert, C., Contreras, R., and Chen, C. (2007). Nonclassical export pathway: overexpression of NCE102 reduces protein and DNA damage and prolongs lifespan in an SGS1 deficient Saccharomyces cerevisiae. Biogerontology *8*, 527–535.
53. Zakrajšek, T., Raspor, P., and Jamnik, P. (2011). Saccharomyces cerevisiae in the stationary phase as a model organism–characterization at cellular and proteome level. J. Proteomics *74*, 2837–2845.
54. Vicens, Q., Kieft, J.S., and Rissland, O.S. (2018). Revisiting the Closed-Loop Model and the Nature of mRNA 5′-3′ Communication. Mol. Cell *72*, 805–812.
55. DeRisi, J.L., Iyer, V.R., and Brown, P.O. (1997). Exploring the metabolic and genetic control of gene expression on a genomic scale. Science *278*, 680–686.
56. Nagalakshmi, U., Wang, Z., Waern, K., Shou, C., Raha, D., Gerstein, M., and Snyder, M. (2008). The transcriptional landscape of the yeast genome defined by RNA sequencing. Science *320*, 1344–1349.
57. Ho, B., Baryshnikova, A., and Brown, G.W. (2018). Unification of Protein Abundance Datasets Yields a Quantitative Saccharomyces cerevisiae Proteome. Cell Syst. *6*, 192–205.e3.
58. Fröhlich, F., Moreira, K., Aguilar, P.S., Hubner, N.C., Mann, M., Walter, P., and Walther, T.C. (2009). A genome-wide screen for genes affecting eisosomes reveals Nce102 function in sphingolipid signaling. J. Cell Biol. *185*, 1227–1242.
59. Genuth, N.R., and Barna, M. (2018). Heterogeneity and specialized functions of translation machinery: from genes to organisms. Nat. Rev. Genet. *19*, 431–452.
60. Joo, M., Yeom, J.H., Choi, Y., Jun, H., Song, W., Kim, H.L., Lee, K., and Shin, E. (2022). Specialised ribosomes as versatile regulators of gene expression. RNA Biol. *19*, 1103–1114.
61. Gay, D.M., Lund, A.H., and Jansson, M.D. (2022). Translational control through ribosome heterogeneity and functional specialization. Trends Biochem. Sci. *47*, 66–81.
62. Spahn, C.M., Beckmann, R., Eswar, N., Penczek, P.A., Sali, A., Blobel, G., and Frank, J. (2001). Structure of the 80S ribosome from Saccharomyces cerevisiae–tRNA-ribosome and subunit-subunit interactions. Cell *107*, 373–386.
63. Hanssum, A., Zhong, Z., Rousseau, A., Krzyzosiak, A., Sigurdardottir, A., and Bertolotti, A. (2014). An inducible chaperone adapts proteasome assembly to stress. Mol. Cell *55*, 566–577.
64. Fleischer, T.C., Weaver, C.M., McAfee, K.J., Jennings, J.L., and Link, A.J. (2006). Systematic identification and functional

screens of uncharacterized proteins associated with eukaryotic ribosomal complexes. Genes Dev. *20*, 1294–1307.
65. Panasenko, O.O., Somasekharan, S.P., Villanyi, Z., Zagatti, M., Bezrukov, F., Rashpa, R., Cornut, J., Iqbal, J., Longis, M., Carl, S.H., et al. (2019). Co-translational assembly of proteasome subunits in NOT1-containing assemblysomes. Nat. Struct. Mol. Biol. *26*, 110–120.
66. Inada, T. (2020). Quality controls induced by aberrant translation. Nucleic Acids Res. *48*, 1084–1096.
67. An, H., and Harper, J.W. (2020). Ribosome Abundance Control Via the Ubiquitin-Proteasome System and Autophagy. J. Mol. Biol. *432*, 170–184.
68. Stein, K.C., Kriel, A., and Frydman, J. (2019). Nascent Polypeptide Domain Topology and Elongation Rate Direct the Cotranslational Hierarchy of Hsp70 and TRiC/CCT. Mol. Cell *75*, 1117–1130.e5.
69. Van Dyke, N., Chanchorn, E., and Van Dyke, M.W. (2013). The Saccharomyces cerevisiae protein Stm1p facilitates ribosome preservation during quiescence. Biochem. Biophys. Res. Commun. *430*, 745–750.
70. Shcherbik, N., and Pestov, D.G. (2019). The Impact of Oxidative Stress on Ribosomes: From Injury to Regulation. Cells *8*, 1379.
71. Parenteau, J., Durand, M., Morin, G., Gagnon, J., Lucier, J.F., Wellinger, R.J., Chabot, B., and Elela, S.A. (2011). Introns within ribosomal protein genes regulate the production and function of yeast ribosomes. Cell *147*, 320–331.
72. Vermeersch, L., Perez-Samper, G., Cerulus, B., Jariani, A., Gallone, B., Voordeckers, K., Steensels, J., and Verstrepen, K.J. (2019). On the duration of the microbial lag phase. Curr. Genet. *65*, 721–727.
73. Breeden, L.L., and Tsukiyama, T. (2022). Quiescence in Saccharomyces cerevisiae. Annu. Rev. Genet. *56*, 253–278.
74. Lanze, C.E., Gandra, R.M., Foderaro, J.E., Swenson, K.A., Douglas, L.M., and Konopka, J.B. (2020). Plasma Membrane MCC/Eisosome Domains Promote Stress Resistance in Fungi. Microbiol. Mol. Biol. Rev. *84*, e00063-19.
75. Paz, I., Abramovitz, L., and Choder, M. (1999). Starved Saccharomyces cerevisiae cells have the capacity to support internal initiation of translation. J. Biol. Chem. *274*, 21741–21745.
76. Arribere, J.A., Doudna, J.A., and Gilbert, W.V. (2011). Reconsidering movement of eukaryotic mRNAs between polysomes and P bodies. Mol. Cell *44*, 745–758.
77. Lee, M.V., Topper, S.E., Hubler, S.L., Hose, J., Wenger, C.D., Coon, J.J., and Gasch, A.P. (2011). A dynamic model of proteome changes reveals new roles for transcript alteration in yeast. Mol. Syst. Biol. *7*, 514.
78. Lackner, D.H., Schmidt, M.W., Wu, S., Wolf, D.A., and Bähler, J. (2012). Regulation of transcriptome, translation, and proteome in response to environmental stress in fission yeast. Genome Biol. *13*, R25.
79. Qian, W., Ma, D., Xiao, C., Wang, Z., and Zhang, J. (2012). The genomic landscape and evolutionary resolution of antagonistic pleiotropy in yeast. Cell Rep. *2*, 1399–1410.
80. Langkjaer, R.B., Cliften, P.F., Johnston, M., and Piskur, J. (2003). Yeast genome duplication was followed by asynchronous differentiation of duplicated genes. Nature *421*, 848–852.
81. Ben-Shem, A., Garreau de Loubresse, N., Melnikov, S., Jenner, L., Yusupova, G., and Yusupov, M. (2011). The structure of the eukaryotic ribosome at 3.0 A resolution. Science *334*, 1524–1529.
82. Pulk, A., Liiv, A., Peil, L., Maiväli, U., Nierhaus, K., and Remme, J. (2010). Ribosome reactivation by replacement of damaged proteins. Mol. Microbiol. *75*, 801–814.
83. Mathis, A.D., Naylor, B.C., Carson, R.H., Evans, E., Harwell, J., Knecht, J., Hexem, E., Peelor, F.F., 3rd, Miller, B.F., Hamilton, K.L., et al. (2017). Mechanisms of In Vivo Ribosome Maintenance Change in Response to Nutrient Signals. Mol. Cell. Proteomics *16*, 243–254.
84. Fusco, C.M., Desch, K., Dörrbaum, A.R., Wang, M., Staab, A., Chan, I.C.W., Vail, E., Villeri, V., Langer, J.D., and Schuman, E.M. (2021). Neuronal ribosomes exhibit dynamic and context-dependent exchange of ribosomal proteins. Nat. Commun. *12*, 6127.
85. Ghosh, A., Williams, L.D., Pestov, D.G., and Shcherbik, N. (2020). Proteotoxic stress promotes entrapment of ribosomes and misfolded proteins in a shared cytosolic compartment. Nucleic Acids Res. *48*, 3888–3905.
86. Giardina, B.J., Stanley, B.A., and Chiang, H.L. (2012). Comparative proteomic analysis of transition of saccharomyces cerevisiae from glucose-deficient medium to glucose-rich medium. Proteome Sci. *10*, 40.
87. Polymenis, M., and Aramayo, R. (2015). Translate to divide: small es, Cyrillicontrol of the cell cycle by protein synthesis. Microb. Cell *2*, 94–104.
88. Sun, Y., Zou, P., Jiang, N., Fang, Y., and Liu, G. (2021). Comparative Analysis of the Complete Chloroplast Genomes of Nine Paphiopedilum Species. Front. Genet. *12*, 772415.
89. Defenouillère, Q., Yao, Y., Mouaikel, J., Namane, A., Galopier, A., Decourty, L., Doyen, A., Malabat, C., Saveanu, C., Jacquier, A., and Fromont-Racine, M. (2013). Cdc48-associated complex bound to 60S particles is required for the clearance of aberrant translation products. Proc. Natl. Acad. Sci. USA *110*, 5046–5051.
90. Zhang, Y., Ma, C., Yuan, Y., Zhu, J., Li, N., Chen, C., Wu, S., Yu, L., Lei, J., and Gao, N. (2014). Structural basis for interaction of a cotranslational chaperone with the eukaryotic ribosome. Nat. Struct. Mol. Biol. *21*, 1042–1046.
91. Heyer, E.E., and Moore, M.J. (2016). Redefining the Translational Status of 80S Monosomes. Cell *164*, 757–769.
92. Biever, A., Glock, C., Tushev, G., Ciirdaeva, E., Dalmay, T., Langer, J.D., and Schuman, E.M. (2020). Monosomes actively translate synaptic mRNAs in neuronal processes. Science *367*, eaay4991.
93. Moon, S.L., Morisaki, T., Stasevich, T.J., and Parker, R. (2020). Coupling of translation quality control and mRNA targeting to stress granules. J. Cell Biol. *219*, e202004120.
94. Opitz, N., Schmitt, K., Hofer-Pretz, V., Neumann, B., Krebber, H., Braus, G.H., and Valerius, O. (2017). Capturing the Asc1p/Receptor for Activated C Kinase 1 (RACK1) Microenvironment at the Head Region of the 40S Ribosome with Quantitative BioID in Yeast. Mol. Cell. Proteomics *16*, 2199–2218.
95. Ferretti, M.B., and Karbstein, K. (2019). Does functional specialization of ribosomes really exist? RNA *25*, 521–538.
96. Frey, S., Pool, M., and Seedorf, M. (2001). Scp160p, an RNA-binding, polysome-associated protein, localizes to the endoplasmic reticulum of Saccharomyces cerevisiae in a microtubule-dependent manner. J. Biol. Chem. *276*, 15905–15912.
97. Ghaemmaghami, S., Huh, W.K., Bower, K., Howson, R.W., Belle, A., Dephoure, N., O'Shea, E.K., and Weissman, J.S. (2003). Global analysis of protein expression in yeast. Nature *425*, 737–741.
98. Winzeler, E.A., Shoemaker, D.D., Astromoff, A., Liang, H., Anderson, K., Andre, B., Bangham, R., Benito, R., Boeke, J.D., Bussey, H., et al. (1999). Functional characterization of the S. cerevisiae genome by gene deletion and parallel analysis. Science *285*, 901–906.
99. Halbeisen, R.E., Scherrer, T., and Gerber, A.P. (2009). Affinity purification of ribosomes to access the translatome. Methods *48*, 306–310.
100. Szklarczyk, D., Franceschini, A., Wyder, S., Forslund, K., Heller, D., Huerta-Cepas, J., Simonovic, M., Roth, A., Santos, A., Tsafou, K.P., et al. (2015). STRING v10: protein-protein interaction networks, integrated over the tree of life. Nucleic Acids Res. *43*, D447–D452.
101. Perez-Riverol, Y., Bai, J., Bandla, C., García-Seisdedos, D., Hewapathirana, S., Kamatchinathan, S., Kundu, D.J., Prakash, A., Frericks-Zipper, A., Eisenacher, M., et al. (2022). The PRIDE database resources in 2022: a hub for mass spectrometry-based proteomics evidences. Nucleic Acids Res. *50*, D543–D552.
102. Ashe, M.P., De Long, S.K., and Sachs, A.B. (2000). Glucose depletion rapidly inhibits translation initiation in yeast. Mol. Biol. Cell *11*, 833–848.
103. Livak, K.J., and Schmittgen, T.D. (2001). Analysis of relative gene expression data using real-time quantitative PCR and the 2(-Delta Delta C(T)) Method. Methods *25*, 402–408.
104. Ternan, N.G., Jain, S., Graham, R.L.J., and McMullan, G. (2014). Semiquantitative analysis of clinical heat stress in Clostridium difficile strain 630 using a GeLC/MS workflow with emPAI quantitation. PLoS One *9*, e88960.
105. Rohart, F., Gautier, B., Singh, A., and Lê Cao, K.A. (2017). mixOmics: An R package for 'omics feature selection and multiple data integration. PLoS Comput. Biol. *13*, e1005752.
106. Trivittayasil, V., Tsuta, M., Kokawa, M., Yoshimura, M., Sugiyama, J., Fujita, K., and Shibata, M. (2015). Method of determining the optimal dilution ratio for fluorescence fingerprint of food constituents. Biosci. Biotechnol. Biochem. *79*, 652–657.
107. Szklarczyk, D., and Jensen, L.J. (2015). Protein-protein interaction databases. Methods Mol. Biol. *1278*, 39–56.

STAR★METHODS

KEY RESOURCES TABLE

REAGENT or RESOURCE	SOURCE	IDENTIFIER
Antibodies		
(HRP)-conjugated primary antibody to Protein A	Abcam	Cat#: ab18596; RRID: AB_777481
Anti-HA (F-7)	Santa Cruz	Cat#: sc-7392; RRID: AB_627809
Anti-GST (B-14)	Santa Cruz	Cat#: sc-138; RRID: AB_627677
Anti-Puromycin- clon 12D10	Sigma-Aldrich	Cat#: MABE 343; N/A
PGK1 Monoclonal Antibody (22C5D8)	ThermoFisher Scientific	Cat#: 459250; RRID:AB_2532235
Anti-Rps3	Frey et al.[96]	N/A
Anti-Rpl35	Frey et al.[96]	N/A
Anti-Pab1	Hoyle et al.[44]	N/A
Goat Anti-Mouse IgG (whole molecule) Polyclonal Antibody, Horseradish Peroxidase Conjugated	Sigma-Aldrich	Cat#: A4416; RRID:AB_258167
Anti-Rabbit IgG (whole molecule)-Peroxidase antibody produced in goat	Sigma-Aldrich	Cat#: A0545 RRID:AB_257896
Chemicals, peptides, and recombinant proteins		
EDTA-free protease inhibitor cocktail	Calbiochem	Cat: # 539134
TRIzol Reagent	Invitrogen	Cat#: 15596-026
Puromycin dihydrochloride	Sigma-Aldrich	Cat#: P9620
Coelenterazine-h	Promega	Cat#: S2011
Trypsin	Promega	Cat#: V5111
Critical commercial assays		
Glucose (GO) Assay Kit	Sigma-Aldrich	Cat#: GAGO20-1KT
PureYield™ Plasmid Miniprep System	Promega	Cat#: A1223
Cycloheximide	Sigma-Aldrich	Cat#: 239763-M
iTaq™ Universal SYBR® Green One-Step Kit	Bio-Rad	Cat#: 1725150
Deposited data		
Proteomics Identifications (PRIDE)	This study. Project accession: PXD047386	https://www.ebi.ac.uk/pride/ RRID:SCR_003411
Experimental models: Organisms/strains		
S. cerevisiae. BY4741 (WT) *MATa his3 Δ 1 leu2 Δ 0 met15 Δ 0 ura3 Δ 0*	ATCC	ATCC 201388
S. cerevisiae. ENO2-TAP *MATa his3 Δ 1 leu2 Δ 0 met15 Δ 0 ura3 Δ 0 ENO2-TAP :: HIS3*	https://horizondiscovery.com/en Ghaemmaghami et al.[97]	N/A
S. cerevisiae. PDC1-TAP *MATa his3 Δ 1 leu2 Δ 0 met15 Δ 0 ura3 Δ 0 PDC1-TAP :: HIS3*	https://horizondiscovery.com/en Ghaemmaghami et al.[97]	N/A
S. cerevisiae. NCE102-TAP *MATa his3 Δ 1 leu2 Δ 0 met15 Δ 0 ura3 Δ 0 NCE102-TAP :: HIS3*	https://horizondiscovery.com/en Ghaemmaghami et al.[97]	N/A

(*Continued on next page*)

Continued

REAGENT or RESOURCE	SOURCE	IDENTIFIER
S. cerevisiae. HSP26-TAP *MATa his3 Δ 1 leu2 Δ 0 met15 Δ 0 ura3 Δ 0 HSP26 -TAP :: HIS3*	https://horizondiscovery.com/en Ghaemmaghami et al.[97]	N/A
S. cerevisiae. TMA17-TAP *MATa his3 Δ 1 leu2 Δ 0 met15 Δ 0 ura3 Δ 0 TMA17 -TAP :: HIS3*	https://horizondiscovery.com/en Ghaemmaghami et al.[97]	N/A
S. cerevisiae. RPS1A -TAP *MATa his3 Δ 1 leu2 Δ 0 met15 Δ 0 ura3 Δ 0 RPS1A -TAP :: HIS3*	https://horizondiscovery.com/en Ghaemmaghami et al.[97]	N/A
S. cerevisiae. RPS1B-TAP *MATa his3 Δ 1 leu2 Δ 0 met15 Δ 0 ura3 Δ 0 RPS1B -TAP :: HIS3*	https://horizondiscovery.com/en Ghaemmaghami et al.[97]	N/A
S. cerevisiae. RPL1A-TAP *MATa his3 Δ 1 leu2 Δ 0 met15 Δ 0 ura3 Δ 0 RPL1A -TAP :: HIS3*	https://horizondiscovery.com/en Ghaemmaghami et al.[97]	N/A
S. cerevisiae. RPL1B-TAP *MATa his3 Δ 1 leu2 Δ 0 met15 Δ 0 ura3 Δ 0 RPL1B -TAP :: HIS3*	https://horizondiscovery.com/en Ghaemmaghami et al.[97]	N/A
S. cerevisiae. RPL24A-TAP *MATa his3 Δ 1 leu2 Δ 0 met15 Δ 0 ura3 Δ 0 RPL24A -TAP :: HIS3*	https://horizondiscovery.com/en Ghaemmaghami et al.[97]	N/A
S. cerevisiae. RPL24B-TAP *MATa his3 Δ 1 leu2 Δ 0 met15 Δ 0 ura3 Δ 0 RPL24B -TAP :: HIS3*	https://horizondiscovery.com/en Ghaemmaghami et al.[97]	N/A
S. cerevisiae. RPL26A-TAP *MATa his3 Δ 1 leu2 Δ 0 met15 Δ 0 ura3 Δ 0 RPL26A -TAP :: HIS3*	https://horizondiscovery.com/en Ghaemmaghami et al.[97]	N/A
S. cerevisiae. RPL26B-TAP *MATa his3 Δ 1 leu2 Δ 0 met15 Δ 0 ura3 Δ 0 RPL26B -TAP :: HIS3*	https://horizondiscovery.com/en Ghaemmaghami et al.[97]	N/A
S. cerevisiae. RPL8A-TAP *MATa his3 Δ 1 leu2 Δ 0 met15 Δ 0 ura3 Δ 0 RPL8A -TAP :: HIS3*	https://horizondiscovery.com/en Ghaemmaghami et al.[97]	N/A
S. cerevisiae. RPL8B-TAP *MATa his3 Δ 1 leu2 Δ 0 met15 Δ 0 ura3 Δ 0 RPL8B -TAP :: HIS3*	https://horizondiscovery.com/en Ghaemmaghami et al.[97]	N/A
S. cerevisiae. RPP2A-TAP *MATa his3 Δ 1 leu2 Δ 0 met15 Δ 0 ura3 Δ 0 RPP2A -TAP :: HIS3*	https://horizondiscovery.com/en Ghaemmaghami et al.[97]	N/A
S. cerevisiae. RPP2B-TAP *MATa his3 Δ 1 leu2 Δ 0 met15 Δ 0 ura3 Δ 0 RPP2B -TAP :: HIS3*	https://horizondiscovery.com/en Ghaemmaghami et al.[97]	N/A
S. cerevisiae. RPL13A-TAP *MATa his3 Δ 1 leu2 Δ 0 met15 Δ 0 ura3 Δ 0 RPL13A -TAP :: HIS3*	https://horizondiscovery.com/en Ghaemmaghami et al.[97]	N/A
S. cerevisiae. RPL13B-TAP *MATa his3 Δ 1 leu2 Δ 0 met15 Δ 0 ura3 Δ 0 RPL13B -TAP :: HIS3*	https://horizondiscovery.com/en Ghaemmaghami et al.[97]	N/A

(*Continued on next page*)

Continued

REAGENT or RESOURCE	SOURCE	IDENTIFIER
S. cerevisiae. RPS26A-TAP *MATa his3 Δ 1 leu2 Δ 0 met15 Δ 0 ura3 Δ 0 RPS26A -TAP :: HIS3*	https://horizondiscovery.com/en Ghaemmaghami et al.[97]	N/A
S. cerevisiae. RPS26B-TAP *MATa his3 Δ 1 leu2 Δ 0 met15 Δ 0 ura3 Δ 0 RPS26B -TAP :: HIS3*	https://horizondiscovery.com/en Ghaemmaghami et al.[97]	N/A
S. cerevisiae. ASC1-TAP *MATa his3 Δ 1 leu2 Δ 0 met15 Δ 0 ura3 Δ 0 ASC1-TAP :: HIS3*	https://horizondiscovery.com/en Ghaemmaghami et al.[97]	N/A
S. cerevisiae. Rps 7A-HA Rps7B-GST: MATa leu2-3,112 trp1-1 can1-100 ura3-1 ade2-1 his3-11,15 [phi$^+$] RPS7A-HA::HIS3 RPS7B-GST::TRP1	This paper	N/A
S. cerevisiae. Rpl 16A-GST Rpl6B-HA: MATa leu2-3,112 trp1-1 can1-100 ura3-1 ade2-1 his3-11,15 [phi$^+$] RPL16A-GST::TRP1 RPL16B-HA::HIS3	This paper	N/A
S. cerevisiae. rps12Δ BY4741 rps12::KanMX4	https://horizondiscovery.com/en Winzeler et al.[98]	N/A
S. cerevisiae. rpl38Δ BY4741 rpl38::KanMX4	https://horizondiscovery.com/en Winzeler et al.[98]	N/A
S. cerevisiae. rpp2aΔ BY4741 rpp2a::KanMX4	https://horizondiscovery.com/en Winzeler et al.[98]	N/A
S. cerevisiae. rpp2bΔ BY4741 rpp2b::KanMX4	https://horizondiscovery.com/en Winzeler et al.[98]	N/A
S. cerevisiae. rps7aΔ BY4741 rps7a::KanMX4	https://horizondiscovery.com/en Winzeler et al.[98]	N/A
S. cerevisiae. rps7bΔ BY4741 rps7b::KanMX4	https://horizondiscovery.com/en Winzeler et al.[98]	N/A
S. cerevisiae. rpl16aΔ BY4741 rpl16a::KanMX4	https://horizondiscovery.com/en Winzeler et al.[98]	N/A
S. cerevisiae. rpl16aΔ BY4741 rpl16b::KanMX4	https://horizondiscovery.com/en Winzeler et al.[98]	N/A
S. cerevisiae. rpl37aΔ BY4741 rpl37a::KanMX4	https://horizondiscovery.com/en Winzeler et al.[98]	N/A
S. cerevisiae. rpl37bΔ BY4741 rpl37b::KanMX4	https://horizondiscovery.com/en Winzeler et al.[98]	N/A
S. cerevisiae. Rpl16A-ZZ BY4741 RPL16A-ZZ::HIS3	Halbeisen et al.[99]	N/A
S. cerevisiae. Rpl16B-ZZ BY4741 RPL16A-ZZ::HIS3	Halbeisen et al.[99]	N/A
Oligonucleotides		
See Table S5 for primers used in this study.	N/A	N/A
Recombinant DNA		
pKK3700	Ferretti, Ghalei et al.[30]	N/A
pFA6a-3HA-HIS3Mx6	Dr. Frydman Lab, Stanford University	Addgene #41600
pFA6a-GST-TRP1	Dr. Frydman Lab, Stanford University	Addgene #41603

(*Continued on next page*)

Continued

REAGENT or RESOURCE	SOURCE	IDENTIFIER
Software and algorithms		
Image J	https://imagej.net/ij/	RRID:SCR_003070
Graphpad Prism 8	https://www.graphpad.com/	RRID:SCR_002798
Proteome Discoverer software, version 2.1.1.21	Thermo Scientific	N/A
XCalibur 3.0.63	Thermo Scientific	N/A
STRING 11.0	(https://stringdb.org/) Szklarczyk et al.[100]	RRID:SCR_005223
Biorender	https://www.biorender.com/b	RRID:SCR_018361

RESOURCE AVAILABILITY

Lead contact

Further information and requests for resources and reagents should be directed to and will be fulfilled by the lead contact, Paula Portela (pportela@qb.fcen.uba.ar).

Materials availability

This study did not generate new unique reagents. All yeast strains generated in this study are available on request to the lead contact.

Data and code availability

- The mass spectrometry proteomics data that support the findings of this study have been deposited to the ProteomeXchange Consortium via the PRIDE[101] partner repository with the dataset identifier PXD04386.
- This paper does not report original code.
- Any additional information required to reanalyze the data reported in this paper is available from the lead contact upon request.

EXPERIMENTAL MODEL AND STUDY PARTICIPANT DETAILS

Yeast strains

The experiments were performed in the *Saccharomyces cerevisiae* strains listed in the key resources table. Genome-edited strains were constructed by genomic recombination.

Growth conditions

Yeast strains were cultured at 30°C in a complete synthetic medium with 2% glucose (SDC). Growth was followed by absorbance measurement at 600 nm (OD600). Cells in exponential phase were obtained when the cultures attained OD600 0.4-0.6 on SDC medium. Cells in stationary phase were obtained by growth on SDC for 72 h. Stationary phase cells were collected by centrifugation, resuspended in the same volume of fresh SDC medium, and incubated at 30°C for different times. Aliquots were taken at indicated times after stimulation with SDC fresh medium. Glucose concentration was determined by the enzymatic method using Glucose (GO) Assay Kit (Sigma). The growth curve was performed in SDC medium. Logistic population growth adjustment was made with Graphpad Prism 8. Y0, initial population = OD600 0.1, [0.043-0.16]. YM, maximum population = OD600 8.9, [8.5-9.2], k = 0.28 h^{-1}, [0.24-0.31], X_{int}, length of lag phase= 3.6 h, [3.2-4.2]. R^2 = 0.99.

METHOD DETAILS

Crude extract preparation

Cells were lysed with glass beads three times for 5 min at 2 min intervals. Lysis was performed at 4 °C in PBS with EDTA-free protease inhibitor cocktail (Calbiochem) and 1 mM phenylmethylsulfonyl fluoride (PMSF). Cell debris was removed by centrifugation. The supernatant was treated with 4x Cracking Buffer (200 mM Tris-HCl pH 6.8, 8 % SDS 0.4 % bromophenol blue, 40 % glycerol, 400 mM 2-mercaptoethanol). Samples were denatured 5 min at 95°C, resolved by SDS-PAGE and further analyzed by Western blot.

Serial dilution assay

Same amount of yeast cells was spotted on SDC media plates by serial 10-fold dilutions and incubated at 30°C. The plates were photographed after 24 and 48 hours.

Puromycin incorporation assay

Puromycin was added directly to stationary cultures at a final concentration of 1 mg/ml and incubated for 1 hour at 30°C. Then, cells were pelleted and resuspended in fresh medium plus 1 mg/ml of puromycin. Post-fresh media aliquots (2 OD_{600nm} cells) were harvested at different times, centrifugated and lysed by alkaline lysis. The cell pellets were suspended in 200 μl of water plus 200 μl of 0.02 M NaOH. After incubation for 8 min. at room temperature, the extracts were centrifugated and the pellets were resuspended in SDS cracking buffer (60 mM Tris-HCl, pH 6.8, 10% glycerol, 2% SDS, 0.01% bromophenol blue, and 5% β-mercaptoethanol) and heated at 100°C for 3 min. The samples were resolved by SDS-PAGE and Western blot.

Western blot analysis

TAP-tagged proteins were detected with a horseradish peroxidase (HRP)-conjugated primary antibody to Protein A (Abcam). HA and GST-tagged proteins were detected with antibodies against HA and GST tags (Santa Cruz). Puromycin-label proteins were detected with antibodies against puromycin (Sigma-Aldrich MABE 343). Equal sample loading was detected by 3-phosphoglycerate kinase level using antibodies against Pgk1 (generously provided by Zaremberg V).

Antibodies against Rps3 and Rpl35 were obtained from Frey & Pool, 2001 and detected with an HRP-conjugated rabbit secondary antibody. Antibodies against Pab1 were obtained from Hoyle et al.,[44] and detected with HRP-conjugated mouse secondary antibody. The immunoblots shown are representative of n=2 biological replicates. Primary antibodies were detected with HRP-conjugated mouse and rabbit secondary antibodies, respectively. Quantification was performed by densitometry using *Image J* on short exposures from two independent experiments.

Protein half-life analysis

Strains ENO2-TAP, PDC1-TAP and NCE102-TAP were used to estimate protein half-life. Cycloheximide Chase Analysis of Protein Degradation was described elsewhere.[43] Briefly, 15 OD_{600} units were collected per time point. Cell pellets were resuspended in 5 ml of their own medium. The cultures were placed at 30°C with 15 mg/ml cycloheximide (CHX). Aliquots of 950 μl were taken at different time points (0, 30, 60, 90 and 120 min) and added to tubes containing 50 μl of 20x Stop Mix (200 mM sodium azide, 5 mg/ml bovine seroalbumin) on ice. Cells were harvested and crude extracts were made as described above. Aliquots of extracts were analyzed by SDS/PAGE and Western blot as described above.

Strains construction

The Rps7A-HA Rps7B-GST strain was constructed using the cellular repair machinery to incorporate the PCR fragment into the *RPS7A* and *RPS7B* gene loci. A fragment containing the C-terminal coding region of *RPS7A* and *RPS7B* genes fused to HA or GST respectively, carrying *HIS3* or *TRP1* selectable markers were amplified by PCR from pFA6a-3HA-HIS3x6 and pFA6a-GST-TRP1 plasmids (generously provided by Dr. Frydman Lab, Stanford University). The epitope tagging was confirmed by PCR and the expression of the tagged protein was monitored by Western blot. The primers used are listed in key resources table "oligonucleotides".

Sucrose cushions analysis

Sucrose cushions protocol were performed as described previously.[99] Briefly, cells were grown at stationary phase and stimulated with fresh media for 60 min. 0.1 mg/ml cycloheximide was added and the cells were lysed with glass beads. A total of 0.3 ml of pre-cleared lysate was loaded onto a total of 3.5 ml of 0.5 M sucrose. After centrifugation for 1 hour at 40.000 r.p.m. using an SW55Ti rotor (Beckman), aliquots from supernatant and pellets were solved on SDS-PAGE and the protein fractionation was evaluated by Western blot.

Ribosome co-sedimentation analysis

Analysis of ribosomal distribution in sucrose density gradients was performed as previously described.[102] 120 OD_{600} units were used per cell extract in stationary phase or after stimulation with SDC fresh medium for 30 min or 60 min. The cultures were added to tubes containing 8 μl/OD unit of cold 10 mg/ml CHX and incubated on ice for 30 min. Cells were harvested by centrifugation and lysed with glass beads. Four A_{260} units of pre-cleared lysate were loaded onto 15–50% linear sucrose gradients. After centrifugation for 2.5 h at 40,000 rpm using a SW41Ti rotor (Beckman), the gradients were fractionated from the top. The A_{254nm} was measured continuously generating the traces shown in the figures using an ISCO UA6 gradient collection apparatus. Individual gradient fractions were collected and samples were used for protein precipitation or RNA extractions as described previously.[38]

Proteins were precipitated with 10% (v/v) trichloroacetic acid, pellets were washed twice with acetone and dried at room temperature. For mass spectrometry, pellets were resuspended in rehydration buffer (8 M urea, 2% NP-40, bromophenol Blue and 10 mM DTT). For Western blot, protein pellets were resuspended in cracking buffer (Tris-HCl 0.06 M pH: 6.8, SDS 2%, β-mercaptoethanol 2.5%, DTT 0.07M, bromophenol blue and glycerol 10%). In both protocols, the samples were pooled according to whether they came from ribosome free fractions, monosomal fractions (40S, 60S and 80S) or polysomal fractions. For RNA extraction of sucrose gradient samples, a standard Trizol Reagent (Life Technologies, Carlsbad, CA) protocol was used. 4 ng of polyadenylated luciferase control mRNA (Promega) were added per fraction. RNA samples from ribosomal free fractions, monosomal (40S, 60S and 80S) or polysomal fractions were pooled. Samples were treated with DNAse (Promega). The absence of DNA in the RNA samples was verified by PCR.

Purification of ribosomes containing Rpl16A-GST

Cultures of stationary yeast cells after stimulation with SDC fresh medium for 60 min were collected and 8 μl/OD unit of cold 10 mg/ml CHX was added and incubated on ice for 30 min. Cells were harvested by centrifugation and lysed using glass beads in a buffer containing 20 mM HEPES pH 7.4, 2 mM magnesium acetate, 100 mM potassium acetate, 0.1 mg/ml CHX, 0.5 mM dithiothreitol. Clarified crude extracts were incubated with GST-Sepharose 4B (Amersham, GE) on a head-over-tail rotator for 2 hours at 4°C. Beads were washed 3 times at 4°C for 5 min with buffer (20 mM Tris pH 7.5, 200 mM NaCl, 15 mM $MgCl_2$, 100 μg/ml CHX, 1% NP-40). After the final wash, the purified ribosomes were eluted with 50 mM glutathione. The samples were precipitated by the addition of 20% TCA and analyzed by Western blot.

RT-qPCR

For Renilla mRNA level determinations, aliquots of 300 ng of RNA were reverse-transcribed into single-stranded cDNA using an oligo-dT primer and M-MLV Reverse Transcriptase (Promega). The cDNAs were amplified by qPCR using gene-specific primers. A SYBR Green real-time quantitative PCR (qPCR) analysis was performed with 1 μg cDNA, 1 μM primers, and SYBR Green qPCR mix (Thermo Fisher Scientific). The real-time qPCR reactions were performed on the StepOne system (Applied Biosystems). For the results shown in Figure S9C the reactions were standardized with the endogenous control of the *POL1* mRNA gene.

We found a statistically significant link between the time course of nutrient stimulation of quiescent cells and the expression of *MRM2*, *TOM1*, and *TPK3*, as well as other housekeeping genes like *POL1* and *TBP*. Therefore, we used the $2^{-\Delta CT'}$ method.[103] Renilla luciferase mRNA levels were measured by qRT-PCR and showed to be similar in wild type and mutant yeast strains in all growth conditions analyzed (Figures S9B and S9C). The primers used are listed in key resources table "oligonucleotides". mRNA distribution across sucrose gradient was analyzed by RT-qPCR performed with 300 ng of RNA with the CFx Connect Real-Time system and the iTaq Universal SYBR Green One Step Kit (Bio-Rad). The sum of the relative abundance levels obtained in the ribosome-free, monosomal and polysomal fractions was taken as 100%, and the percentage of distribution of each mRNA in the fractions in each condition was calculated. The experiment was carried out in three biological replicates (Figure 1C).

Renilla luciferase assay

Cells were transformed with a plasmid encoding Renilla luciferase pKK3700[30] and grown on leucine minus selective media. For the Renilla luciferase assay, stationary phase cultures were stimulated for 60, 120, and 180 min with fresh SDC media or growth to the exponential phase of growth. Cells were harvested by centrifugation, washed once with 1 ml of ice-cold lysis buffer (PBS pH 7.4, 1 mM PMSF) and then resuspended in 0.3 mL of the same buffer. Cells were lysed with glass beads and processed as described above. Protein concentrations were determined by the Bradford method. Renilla luciferase activity was measured using 0.1–2 μl of crude extract and 1 μl of coelenterazine H 50 mM (Promega) in the Glomax Multi-detection System (Promega).

Sample preparation and mass spectrometry

27 samples corresponding to SP (stationary phase), SP+SDC 30 min (stationary phase cells incubated during 30 min with fresh SDC medium); SP+SDC 60 min (stationary phase cells incubated during 60 min with fresh SDC medium) were fractionated in F (Free), M (monosome fractions 80S + 60S + 40S) and P (polysome fractions) n=3 biological replicates. The samples were mixed with cracking buffer and equivalent protein amounts of each fraction were left to migrate for 1 cm into the 10% PAGE-SDS. Proteins were fixed with 30% (v/v) ethanol and 2% (v/v) phosphoric acid. Protein bands (1cm x 1cm) containing the whole protein fraction loaded in each well were excised from the gels and analyzed by mass spectrometry. Protein digestion and mass spectrometry analysis were performed at the Proteomics Core Facility CEQUIBIEM, at the University of Buenos Aires/CONICET (National Research Council). SDS-PAGE gel excised protein bands were sequentially washed and destained with 50 mM ammonium bicarbonate pH=8, 25 mM ammonium bicarbonate 50% acetonitrile, and 100% acetonitrile; reduced with 10 mM DTT at 56°C 45 min and alkylated with 50 mM iodoacetamide at room temperature in the dark for 60 min, and in-gel digested with 100 ng Trypsin (Promega V5111) in 25 mM ammonium bicarbonate overnight at 37°C. Peptides were recovered by elution with 50% acetonitrile-0.5% trifluoroacetic acid at room temperature, including brief sonication, and further concentrated by speed-vacuum drying. Samples were resuspended in 15 μl of water containing 0.1% Formic Acid and desalted with ZipTip C18 columns (Millipore). The digests were analyzed by nanoLC-MS/MS in a Thermo Scientific QExactive Mass Spectrometer coupled to a nanoHPLC EASY-nLC 1000 (Thermo Scientific). For the LC-MS/MS analysis, approximately 1 μg of peptides was loaded onto the column and eluted for 120 min using a reverse phase column (C18, 2 μm, 100 A, 50 μm x 150 mm) Easy-Spray Column PepMap RSLC-P/N ES801) suitable for separating complex peptide mixtures with a high degree of resolution. The flow rate used for the nano column was 300 nL.min-1 and the solvent range from 7% B (5 min) to 35% (120 min). Solvent A was 0.1% formic acid in water and solvent B was 0.1% formic acid in acetonitrile. The injection volume was 2 μL. The MS equipment has a high collision dissociation cell (HCD) for fragmentation and an Orbitrap analyzer (Thermo Scientific, Q-Exactive). A voltage of 3,5 kV was used for Electro Spray Ionization (Thermo Scientific, EASY-SPRAY). XCalibur 3.0.63 (Thermo Scientific) software was used for data acquisition. Equipment configuration allows peptide identification at the same time of their chromatographic separation. Full-scan mass spectra were acquired in the Orbitrap analyzer. The scanned mass range was 400-1800 m/z, at a resolution of 70.000 at 400 m/z and the 15 most intense ions in each cycle, were sequentially isolated, fragmented by HCD and MS/MS spectra were measured in the Orbitrap analyzer. Peptides with a charge of +1 or with unassigned charge state were excluded from MS2 fragmentation.

Analysis of mass spectrometry spectra

Q-Exactive raw data was processed using Proteome Discoverer software (version 2.1.1.21 Thermo Scientific) and searched against *Saccharomyces cerevisiae* UP00002311 protein sequence database with trypsin specificity and a maximum of one missed cleavage per peptide. Proteome Discoverer searches were performed with a precursor mass tolerance of 10 ppm and product ion tolerance to 0.05 Da. Static modifications were set to carbamidomethylation of Cys, and dynamic modifications were set to oxidation of Met and protein N-terminal acetylation. Protein hits were filtered for high confidence peptide matches, with a maximum protein and peptide false discovery rate of 1% calculated by employing a reverse database strategy.

A total of 513 proteins were identified. The list of hits was filtered with the following requirement: proteins should have at least 2 high confidence peptides and should add up to, at least, 5 PSMs (Peptide spectrum Matches) among the three biological replicates of a given condition. This filtering criteria is based on a previous study performed at the CEQUIBIEM facility, where three methodological replicates of *S. cerevisiae* crude extract tryptic digests were injected three times each (technical replicates) in the Mass Spectrometer. This study showed that when the sum of the PSMs of the three technical replicates is less than five for a given protein, this protein might not be detected in other methodological replicates, due to low abundance of the protein and the stochastic nature of the technique.

For quantitative analysis Proteome Discoverer calculates the area under the curve of the 3 most intense MS peaks for each protein in each condition. Total areas for each of the 27 samples were calculated by adding the areas of all identified proteins in each sample; and these values were used to normalize the area value of the individual proteins.

The abundance of ribosomal proteins in stationary phase (SP) and post stimulus (SP+60 min SDC) was calculated by searching the raw files of the free, monosome and polysome fractions together, using Proteome Discoverer. Total areas were calculated for each of the 6 samples and these values were used to normalize the area value of the individual proteins.

To determine the change in the distribution of protein abundance between the free, monosomal, and polysomal fractions corresponding to the quiescence conditions and 60 min after resuspension in fresh medium the exponentially modified protein abundance index (emPAI)[104] was used. The data was used to calculate M%= [emPAI protein x / Σ emPAI (sum of emPAI values for all proteins identified in each sample)]*100.

A multivariate discriminant analysis was performed to determine the discriminant variables of the riboproteome composition using the mixOmics R package, perform partial least squares discriminant analysis (PLS-DA).[105] It was differentiated based on condition (SP, SP + 30 min SDC, SP + 60 min SDC), fraction type (Free, Monosomal, or Polysomes), or both. The best possible number of variables was used for the first two analyses. The best number of variables (normalised protean areas) for the first two analyses were chosen using the misclassification error rate calculated using the leave-one-out or stratified cross-validation methods. The number of variables was maximized in the PLS-DA where discrimination was done according to fraction and condition.[106]

String analysis

The data was analyzed using STRING 11.0 (https://stringdb.org/).[107] Each node represents a protein found by nanoLC-MS / MS. The colours of the nodes indicate the category of *Gene Ontology* to which the protein belongs; some belong to more than one category and therefore are represented with more than one colour. The *Gene Ontology categories* that best describe the networks obtained are shown. The lines connecting nodes indicate protein interactions, which does not necessarily imply physical interaction between them. The thickness of the line that joins two nodes indicates the confidence of the association. This software uses as evidence of interaction the data of: *text mining*, databases of protein-protein interactions, co-expression, *neighbourhood*, gene fusion, and co-occurrence.

QUANTIFICATION AND STATISTICAL ANALYSIS

The results are expressed as the mean $\pm$ SE. The averaged variables were compared using the unpaired t-test, the one-way ANOVA test, and Tukey's test for multiple comparisons. Time course data were analyzed using a two-way ANOVA with a Bonferroni multiple comparison test. P-values of less than 0.05 were considered statistically significant. The growth curves were analyzed using a logistic population growth adjustment. Graphpad Prism 8 was used for statistical analysis.